CHARGE EXCHANGE AND EXCITATION IN COLLISIONS OF HEAVY-ELEMENT IMPURITY IONS WITH HELIUM ATOMS AND ALPHA PARTICLES IN FUSION REACTORS

V. K. Nikulin and N. A. Guschina

Division of Plasma Physics, Atomic Physics and Astrophysics of the Ioffe Physical Technical Institute, Russia

Research Co-ordination Meeting

on C R P

“ Atomic data for heavy element impurities

in fusion reactors”

4–6 March 2009, IAEA, Vienna, Austria

OUTLINE:

1. **SUMMARY**
2. **CITATION OF PERIODICAL REPORTING WORK DONE UNDER CRP**
3. **THEORETICAL METHOD**
4. **CALCULATION OF CHARGE EXCHANGE, TRANSFER EXCITATION AND EXCITATION CROSS SECTIONS IN COLLISIONS OF Ti^{4+}, Si^{4+}, Cr^{6+}, Fe^{8+}, Ni^{6+}, Cu^{6+}, Mo^{6+}, AND W^{6+} WITH HELIUM ATOMS IN THE GROUND STATE**
5. **THEORETICAL STUDY OF THE SINGLE–ELECTRON CAPTURE AND EXCITATION PROCESSES IN COLLISIONS OF Ti^{4+}, Cr^{6+} AND Fe^{8+} WITH HELIUM ATOMS IN THE METASTABLE STATE**
6. **STUDY OF ALPHA PARTICLES NEUTRALIZATION THROUGH QUASI–RESONANT DOUBLE ELECTRON CAPTURE IN SLOW COLLISIONS WITH C^{2+} AND Ti^{2+} IONS**
7. **ELECTRON CAPTURE AND EXCITATION PROCESSES IN COLLISIONS OF ALPHA PARTICLES WITH Be–LIKE OXYGEN IONS**
8. **THEORETICAL STUDY OF CHARGE TRANSFER AND EXCITATION IN SLOW COLLISIONS BETWEEN Bi^{4+} IONS IN THE GROUND AND METASTABLE STATES**

Summary

Theoretical data for heavy-element impurities obtained in accordance with the Coordinated Research Project are considered. New data on the partial and total cross sections of single and double electron capture, transfer excitation and excitation in collisions of impurity ions Ti^{4+}, Si^{4+}, Cr^{6+}, Fe^{8+}, Ni^{6+}, Cu^{6+}, Mo^{6+}, and W^{6+} with helium atoms in the ground state were obtained in the energy range of impurity ions 4 – 800 keV. The partial and total cross sections of electron capture into n-shells of Ti^{3+} (n=5–8), Cr^{5+} (n=6–9), and Fe^{7+} (n=8–11) were calculated for the first time in collisions of the impurity ions with helium atoms in metastable states.

The cross sections of the alpha particle neutralization through the quasi-resonant double electron capture into ground ($1s^2$) and metastable ($1sn\ell$) states of He atoms in their slow collisions with C^{2+} and Ti^{2+} ions were calculated (for Ti^{2+} for the first time).

Data on the partial and total cross sections for the single electron capture and target excitation in collisions of alpha particles with the Be-like oxygen ions were obtained in the high energy range 0.2 – 2 MeV.

Data for charge exchange and excitations in collisions due to betatron oscillations in the ion beams between the Bi^{4+} ions in the ground (6s) and metastable (6p) states were obtained. The fraction of metastable ions in the beams was estimated by comparison of our theoretical data with the Giessen experimental results for the total charge exchange cross sections. This fraction is vital to designing accelerators.

Calculations of the charge exchange and excitation cross sections in ion-atom collisions were carried out in the framework of the close-coupling equation method involving basis of the many-electron quasimolecular states.

Citation of periodical reporting work done under CRP

[1] V. K. Nikulin, N. A. Guschina. *Electron transfer and excitation in collisions between heavy element impurity ions and helium atoms. I.* Ti^{4+} *– He collisions.* Report of Ioffe Physico-Technical Institute N 1789 (2006) 23 p.

[2] V. K. Nikulin, N. A. Guschina. *Electron transfer and excitation in collisions between* Ti^{4+}, Cr^{6+} *ions and helium atoms.* Report of Ioffe Physico-Technical Institute N 1791 (2006) 45 p.

[3] V. K. Nikulin, N. A. Guschina. *Electron transfer and excitation in collisions between* Fe^{8+} *ions and helium atoms.* Report of Ioffe Physico-Technical Institute N 1792 (2007) 27 p.

[4] V. K. Nikulin, N. A. Guschina. *State-selective and total electron transfer and excitation cross sections in slow collisions of excited He(1s2s) atoms and* Ti^{4+}, Cr^{6+}, Fe^{8+} *ions. I.* Ti^{4+}*– He(1s2s) collision.* Report of Ioffe Physico-Technical Institute N 1793 (2007) 35 p.

[5] V. K. Nikulin, N. A. Guschina. *State-selective and total electron transfer and excitation cross sections in slow collisions of excited He(1s2s) atoms and* Ti^{4+}, Cr^{6+}, Fe^{8+} *ions. II.* Cr^{6+}, Fe^{8+}*– He(1s2s) collisions.* Report of Ioffe Physico-Technical Institute N 1794 (2007) 34 p.

[6] V. K. Nikulin, N. A. Guschina. *Cross sections for charge transfer and excitation in alpha-particle collisions with Be-like oxygen impurity ions in plasma.* **Technical Physics**, 51, 1276 (2006).

[7] V. K. Nikulin, N. A. Guschina. *Single-electron charge transfer and excitations at collisions between* Bi^{4+} *ions in the kiloelectronvolt energy range.* **Technical Physics**, 52, 148 (2007).

[8] V. K. Nikulin, N. A. Guschina. *Theoretical study of charge transfer and excitation in slow collisions between* Bi^{4+} *ions in the ground and metastable states.* **XXV ICPEAC, Abstracts**,2007 Mo082.

[9] V. K. Nikulin and N. A. Guschina. *Cross sections for electron capture and excitation processes in collisions between the hydrogen-like* He^{+}*(1s) and* B^{4+}*(1s),* C^{5+}*(1s),* N^{6+}*(1s),* O^{7+}*(1s) ions.* **Atomic and Plasma-Material Interaction Data for Fusion**, 13, 95 (2007).
[10] V. K. Nikulin, N. A. Guschina.*State-selective and total electron transfer cross sections in collisions between heavy metal element ions and helium atoms. I.* $W^{6+} + He$. Report of Ioffe Physico-Technical Institute N 1796 (2008) 39 p.
[11] V. K. Nikulin, N. A. Guschina. *State-selective and total electron transfer cross sections in collisions between heavy metal element ions and helium atoms. II.* $Mo^{6+} + He$. Report of Ioffe Physico-Technical Institute N 1797 (2008) 44 p.
[12] V. K. Nikulin, N. A. Guschina. *State-selective and total electron transfer cross sections in collisions between heavy metal element ions and helium atoms. III.* $Ni^{6+} + He$. Report of Ioffe Physico-Technical Institute N 1798 (2008) 37 p.
[13] V. K. Nikulin, N. A. Guschina. *State-selective and total electron transfer cross sections in collisions between heavy metal element ions and helium atoms. IV.* $Cu^{6+} + He$. Report of Ioffe Physico-Technical Institute N 1800 (2008) 38 p.
[14] V. K. Nikulin, N. A. Guschina. *Alpha particle neutralization at their slow collisions with* Ti^{2+} *ions through quasi-resonant double electron capture.* Report of Ioffe Physico-Technical Institute N 1799 (2008) 43 p.
[15] V. K. Nikulin, N. A. Guschina. *Electron transfer and excitation in collisions between* Si^{4+} *ions and helium atoms.* Report of Ioffe Physico-Technical Institute (2009) in press

3. Theoretical method

The study of charge transfer and excitation reactions was performed by the use of the close-coupling equation method with two- or many-electron quasi-molecular states ϕ_i as a basis. Coulomb trajectories were used to integrate coupled equations using code TANGO provided us by A. Salin [16].
Two-electron wave function ϕ_i for the orthonormal one-electron basis ψ_k may be represented in the form

$$\phi_i(\vec{r}_k, \vec{r}_l) = \frac{1}{\sqrt{2}}[\psi_k(\vec{r}_k)\psi_l(\vec{r}_l) \pm \psi_k(\vec{r}_l)\psi_l(\vec{r}_k)] \quad (\pm - \text{singlet, triplet cases}) \ , \quad (3.1)$$

where ψ_k may be obtained within the effective potential method. Our effective potential [17] takes into account screening of a nucleus by electrons as follows

$$V_{eff}(R, \vec{r}_j) = \frac{1}{2}\left[\frac{a_1 - b_1}{r_{1j}} + \frac{a_1 + b_1}{r_{2j}} + \frac{\tilde{a}_1 + Ra_0}{r_{1j}r_{2j}} + \frac{b_2(r_{1j} - r_{2j})^2}{Rr_{1j}r_{2j}}\right] \quad (3.2)$$

and allows for the separation of variables in the one-electron Schrödinger equation in prolate spheroidal coordinate system

$$h\psi_k(\vec{r}_j) = \left[-\frac{\nabla_j^2}{2} - \frac{Z_1}{r_{1j}} - \frac{Z_2}{r_{2j}} + V_{eff}(\vec{R}, r_{1j}, r_{2j})\right]\psi_k(\vec{r}_j) = \varepsilon_k(R)\psi_k(\vec{r}_j) \ , \quad (3.3)$$

where R is the internuclear distance; r_{1j} and r_{2j} are distances from the $\vec{r}_j$ electron to the nuclei with

charges Z_1 and Z_2, respectively; a_0, $\tilde{a}_1$, a_1, b_1, and b_2 are the effective potential parameters.
If V_{eff}=0, we have the H_2^+ problem and the One Electron Diatomic Molecular Orbitals (OEDMO) with hidden symmetry. In our method Screened Diatomic Molecular Orbitals (SDMO), ψ_k has the same symmetry.
The SDMO basis was used for calculating the total energies E_i, for example of the two-electron or many-electron diabatic states

$$\mathrm{E}_i = <\phi_i|\mathrm{H}|\phi_i> = \varepsilon_k + \varepsilon_l + J_{kl}^c \pm J_{kl}^{ex} - (V_{eff}^k + V_{eff}^l) \; , \tag{3.4}$$

$$\mathrm{H} = \sum_{j=k,l} \left[-\frac{\nabla_j^2}{2} - \frac{Z_1}{r_{1j}} - \frac{Z_2}{r_{2j}} \right] + \frac{1}{r_{kl}} \; . \tag{3.5}$$

Here J_{kl}^c and J_{kl}^{ex} are the Coulomb and exchange integrals; V_{eff}^k and V_{eff}^l are diagonal matrix elements of the effective potential.
The many-electron energies are calculated in fact to the first one order of the perturbation theory in the residual interaction $W=1/r_{kl} - V_{eff}(\vec{r}_k) - V_{eff}(\vec{r}_l)$.
The matrix elements of dynamic and potential couplings are obtained using the calculated basis SDMO. To take into account electron momentum transfer, the matrix elements are calculated for origin placed at centre of charges of colliding ions.

4. Calculation of charge exchange, transfer excitation and excitation cross sections in collisions of Ti^{4+}, Si^{4+}, Cr^{6+}, Fe^{8+}, Ni^{6+}, Cu^{6+}, Mo^{6+}, and W^{6+} with helium atoms in the ground state

The single electron capture (SEC) and double electron capture (DEC), transfer excitation (TE), and excitation (EXC) of helium were calculated at relative keV-collision energies important for modeling and diagnostics of the plasma edge.
Calculations for the Ti^{4+}– He and Si^{4+}– He collisions in the energy range 0.1–6 MeV were performed by Fritsch [18] within the framework of the close-coupling method with regard to two active electrons also, but the important two-electron transfer excitation and DEC channels being omitted.

4.1. Ti^{4+} – He Collision

For comparison with the results of our previous study in the first year [1], more detailed calculations of SEC, TE, DEC and direct helium excitation (EXC) cross sections were recently performed [14] for reactions

$$\mathrm{Ti}^{4+}(3p^6) + \mathrm{He}(1s^2) \rightarrow \begin{cases} \mathrm{Ti}^{3+}(3p^6nl) + \mathrm{He}^+(1s) & \text{(SEC)} \quad (n=3,4) \\ \mathrm{Ti}^{3+}(3p^63d) + \mathrm{He}^+(2p) & \text{(TE)} \\ \mathrm{Ti}^{2+}(3p^63d^2) + \mathrm{He}^{2+} & \text{(DEC)} \\ \mathrm{Ti}^{4+}(3p^6) + \mathrm{He}(1s2l). & \text{(EXC)} \end{cases} \tag{1}$$

The entrance and sixteen exit channels in the reactions (1) are presented in Fig. 1. As distinct from our previous study of this reaction [2], six additional channels were taken into account: SEC(5f, 5g), DEC($3d^2_{\pm1}$), EXC(1s2s, $1s2p_{\pm1}$, $1s3p_0$, $1s3p_{\pm1}$).

Figure 1: The energies $E_i(R)$ of seventeen two-electron states $\phi_i(\psi_j, \psi_{j'})$ of the (Ti^{4+}+He) quasimolecule:

a) the entrance channel (red curve) – $\phi_1(3d\sigma', 3d\sigma')$;

b) the channels of SEC into nl-states with n=3–5 of Ti^{3+}ions – $\phi_{12}(3d\sigma, 4f\sigma)$, $\phi_{13}(3d\sigma, 3d\pi)$; $\phi_{15}(3d\sigma, 4d\sigma)$, $\phi_3(3d\sigma, 6h\sigma)$; $\phi_4(3d\sigma, 6g\sigma)$, $\phi_5(3d\sigma, 7i\sigma)$;

c) the channels of DEC into 3d-states of Ti^{2+} ions – $\phi_{14}(4f\sigma', 4f\sigma')$, $\phi_2(4f\sigma', 3d\pi')$; $\phi_{17}(3d\pi', 3d\pi')$;

d) TE channels (SEC into 3d-states of Ti^{3+} ion with the 1s$\longrightarrow$ 2l, 3l excitation of He atom) – $\phi_{16}(4f\sigma, 5f\sigma)$, $\phi_6(4f\sigma, 5g\sigma)$, $\phi_7(4f\sigma, 4f\pi)$;

e) the channels of electron excitations 1s$\longrightarrow$2s, $2p_{\pm1}$, $3p_0$s, and $3p_{\pm1}$ in He atoms – $\phi_8(3d\sigma, 5f\sigma')$, $\phi_{10}(3d\sigma, 5g\pi')$, $\phi_9(3d\sigma, 8i\sigma')$, $\phi_{11}(3d\sigma, 7h\pi')$.

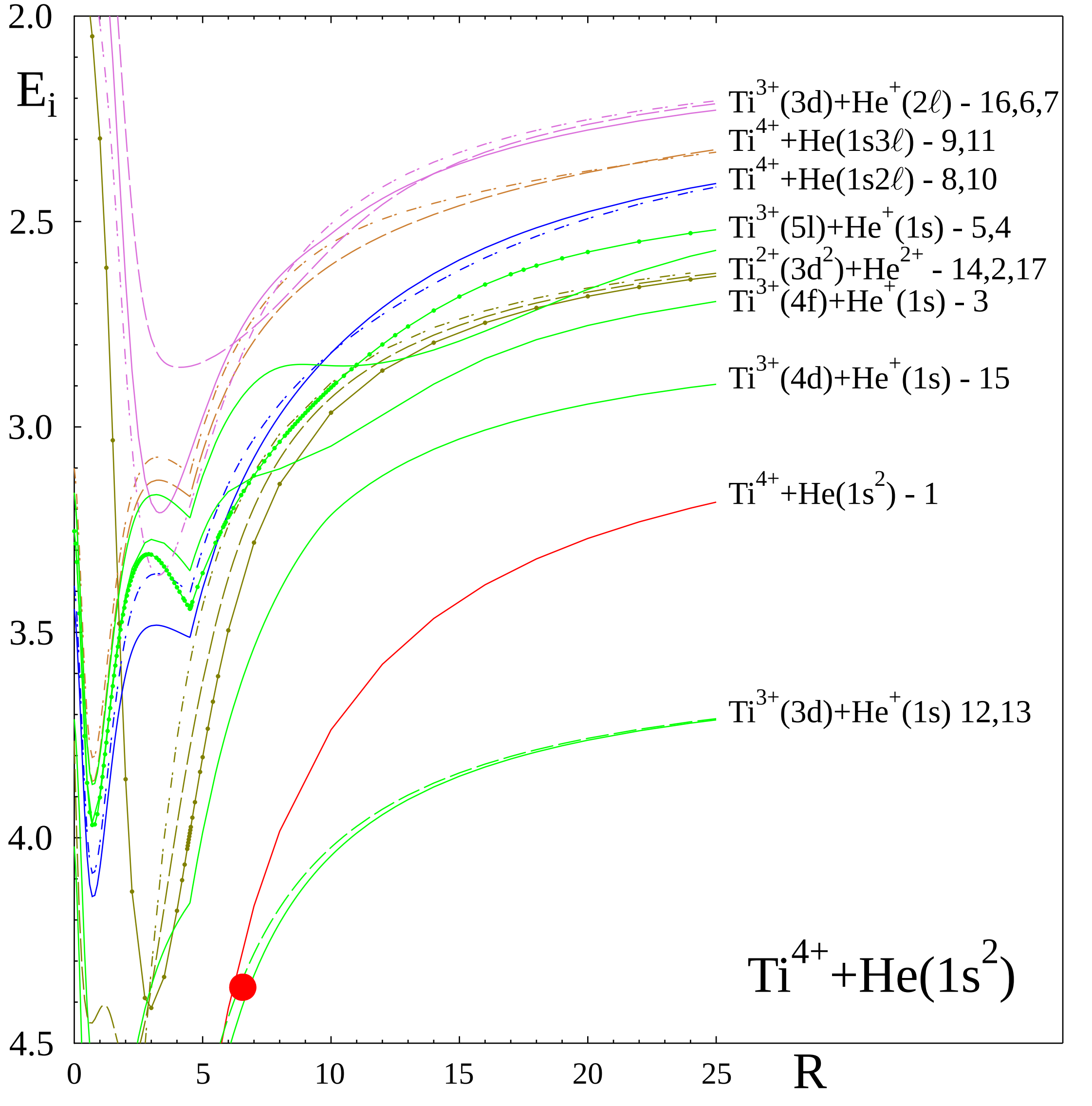

The calculated cross sections as a function of the Ti^{4+} ion energy are shown in Fig. 2 together with the theoretical results by Fritsch [18]. It is clearly seen that our data on SEC agree with the results by Fritsch at energy $\sim$ 100 keV. The electron transfer process in Ti^{4+} – He collisions is seen to populate predominantly the 3d level of projectile. The maximum values of total cross section for excitation of helium to ^{1}2S+^{1}2P states and for DEC were obtained equal 2.6×10^{-16} cm^2 at E_c=400 keV and 1.1×10^{-16} cm^2 at E_c=200 keV in comparison with the values $\sim 5\times10^{-18}$ cm^2 and $\sim 2\times10^{-16}$ cm^2 obtained in our previous study [2] where only the channels of helium excitation into 1s2s and $1s2p_0$ states and DEC into $3d_0^2$ states were taken into account.

Figure 2: The calculated cross sections as a function of the impurity ion energy E_c for Ti^{4+} + He(1s^2) collision: $\sigma(n)$ - SEC cross sections into n shells of Ti^{3+} ions, Σ(SEC) - the total cross section.
Σ'(SEC), $\sigma'(3)$, $\sigma'(4)$ - the results by Fritsch (blue curves).

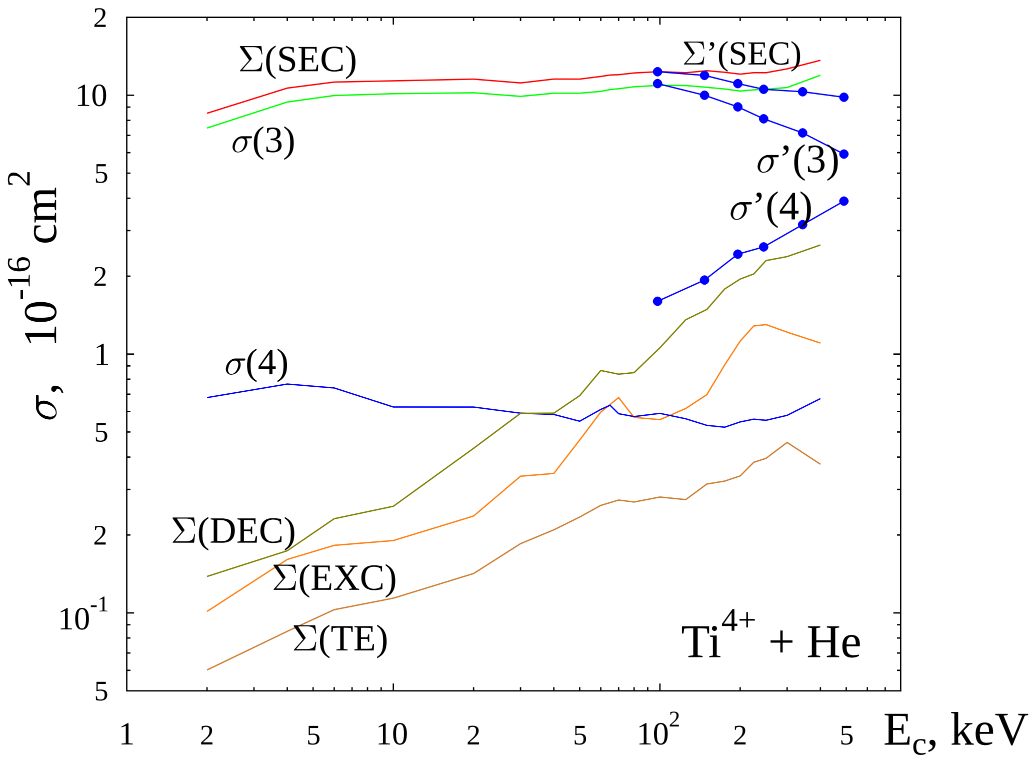

4.2. Si^{4+} – He Collision

The partial and total cross sections for SEC and TE were calculated [15] for reactions

$$Si^{4+}(2p^6) + He(1s^2) \to \begin{cases} Si^{3+}(2p^6 nl) + He^{+}(1s) & (SEC) \quad (n = 3 - 5) \\ Si^{3+}(2p^6 3s) + He^{+}(2s). & (TE) \end{cases} \qquad (2)$$

The nine two-electron quasi-molecular states for reactions (2) are shown in Fig. 3.

Figure 3: The energies $E_i(R)$ of two-electron states $\phi_i(\psi_j, \psi_{j'})$ of the (Si^{4+}+He) quasi-molecule:

a) the entrance channel (red curve) – $\phi_1(3d\sigma, 3d\sigma)$;

b) the channels of SEC the single-electron transfer into $n\ell$-states with n=3–5 of the Si^{3+} ions – $\phi_2 = [3d\sigma, 3p\sigma]$, $\phi_3 = [3d\sigma, 3s\sigma]$, $\phi_4 = [3d\sigma, 4d\sigma]$, $\phi_9 = [3d\sigma, 3p\pi]$; $\phi_5 = [3d\sigma, 4f\sigma]$, $\phi_6 = [3d\sigma, 4p\sigma]$; $\phi_8 = [3d\sigma, 5d\sigma]$;

c) the TE channel – $\phi_7 = [3s\sigma, 5f\sigma]$.

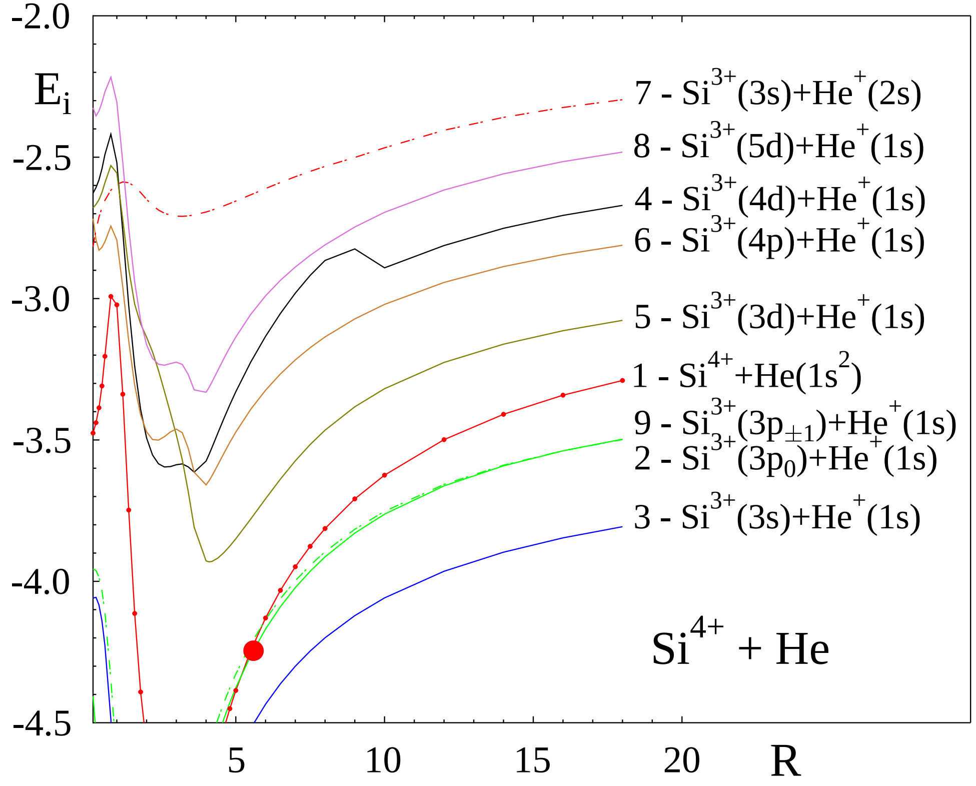

The calculated cross sections as a function of the Si^{4+} ion energy E_c from 2 keV to 300 keV are shown in Fig. 4 together with the SEC cross section obtained by Fritsch [18]. Our data on the total SEC agree with the results by Fritsch at energy $\sim$ 130 keV. SEC into 3ℓ-states of the Si^{3+} dominantes in the overall range of the collision energies. The transfer excitation cross section was obtained less than 10^{-21} cm^2.

Figure 4: The calculated cross sections as a function of the impurity ion energy E_c: $\sigma(n)$ - SEC cross sections into n shells of Si^{3+} ions, Σ(SEC) - the total SEC cross section.
$\Sigma'(SEC)$ - the results by Fritsch [18] (blue curve).

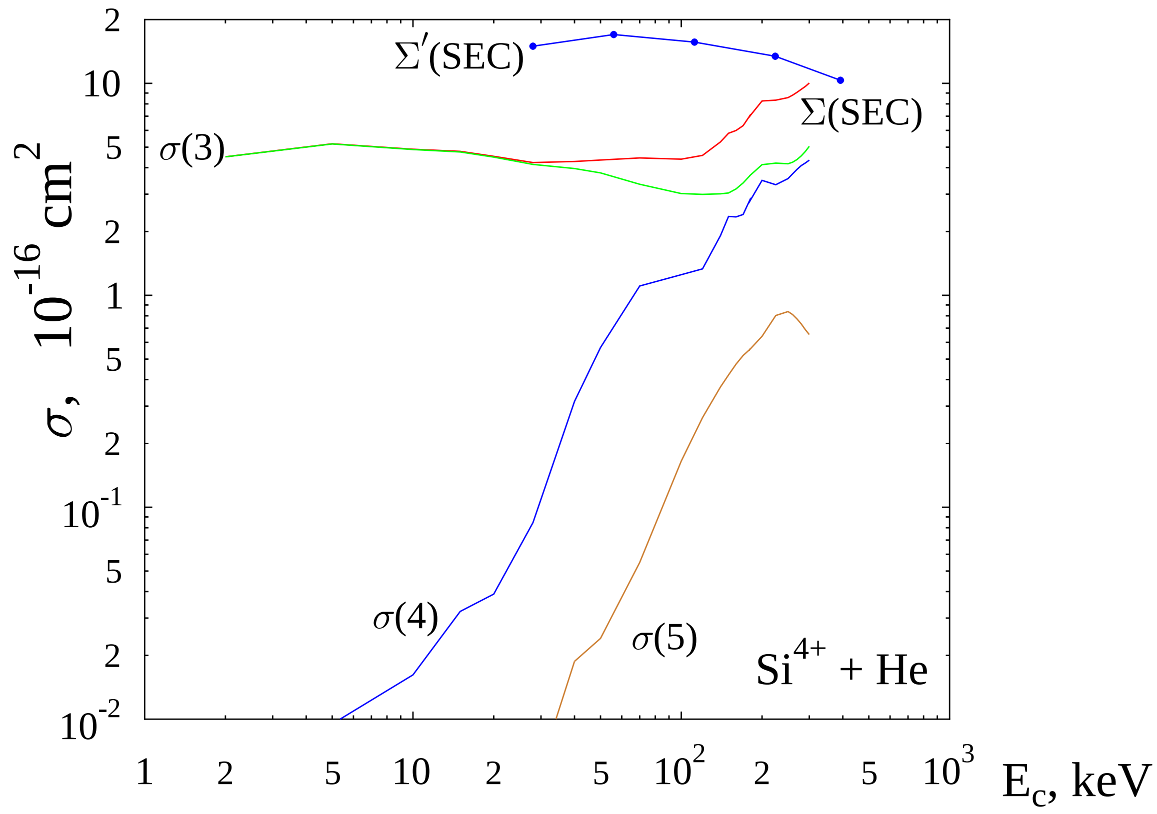

4.3. Cr^{6+} – He Collision

Cross sections for SEC, DEC and TE channels were calculated [2] for the reactions

$$Cr^{6+}(3p^6) + He(1s^2) \rightarrow \begin{cases} Cr^{5+}(3p^6 nl) + He^{+}(1s) & (SEC) \quad (n = 4, 5) \\ Cr^{4+}(3p^6 3d5l) + He^{2+} & (DEC) \\ Cr^{5+}(3p^6 3d) + He^{+}(2l), & (TE) \end{cases} \tag{3}$$

The eleven two-electron quasimolecular states for reactions (3) are shown in Fig. 5.

Figure 5: The energies $E_i(R)$ of the two-electron states $\phi_i(\psi_j, \psi_{j'})$ of the (Cr^{6+}+He) quasimolecule:
a) the entrance channel (red curve) – $\phi_1(4f\sigma', 4f\sigma')$;
b) the channels of SEC into nℓ-states with n=4-5 of Cr^{5+} ions – $\phi_2(4s\sigma, 4f\sigma)$, $\phi_3(4p\sigma, 4f\sigma)$, $\phi_4(4d\sigma, 4f\sigma)$, $\phi_5(5g\sigma, 4f\sigma)$, $\phi_6(4f\pi, 4f\sigma)$, $\phi_7(6g\sigma, 4f\sigma)$, $\phi_8(6h\sigma, 4f\sigma)$;
c) the channels of DEC into 3d5g-state of Cr^{6+} ions – $\phi_9(3d\sigma^*, 6h\sigma^*)$;
d) the TE channels (SEC into 3d-state of Cr^{5+} ion with the 1s→ $2l$ excitation of He atom) – $\phi_{10}(3d\sigma, 7i\sigma)$, $\phi_{11}(3d\sigma, 5f\sigma)$.

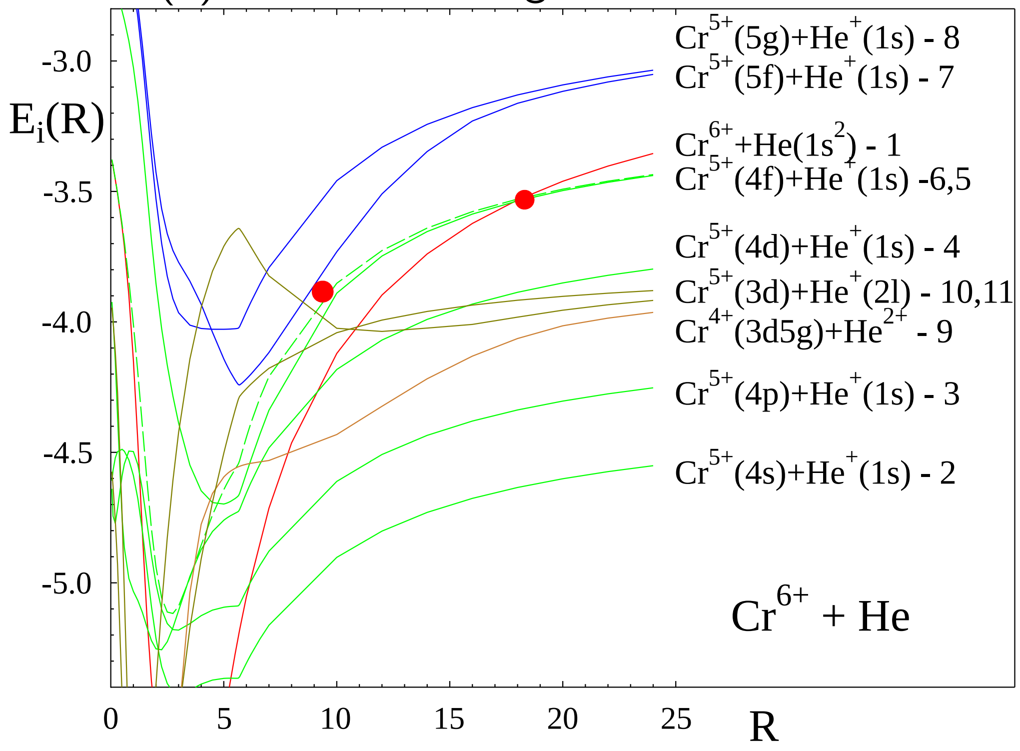

The calculated cross sections for Cr^{6+} + He($1s^2$) in the energy range from 2 to 400 keV are shown in Fig. 6. The maximum value of the total SEC and DEC cross sections obtained is equal to 4.72×10^{-15} cm^2 (at $E_c \simeq$ 400 keV) and 1.45×10^{-16} cm^2 (at $E_c \simeq$ 300 keV).

Figure 6: The calculated cross sections as a function of the impurity ion energy E_c for Cr^{6+} + He collision: Σ(SEC) – the total cross section of SEC + TE; $\sigma(4)$ and $\sigma(5)$ – the cross sections of SEC into n-shells with n=4 and n=5 of Cr^{5+} ions, Σ(TE) – TE cross section; Σ(DEC) – DEC cross section.

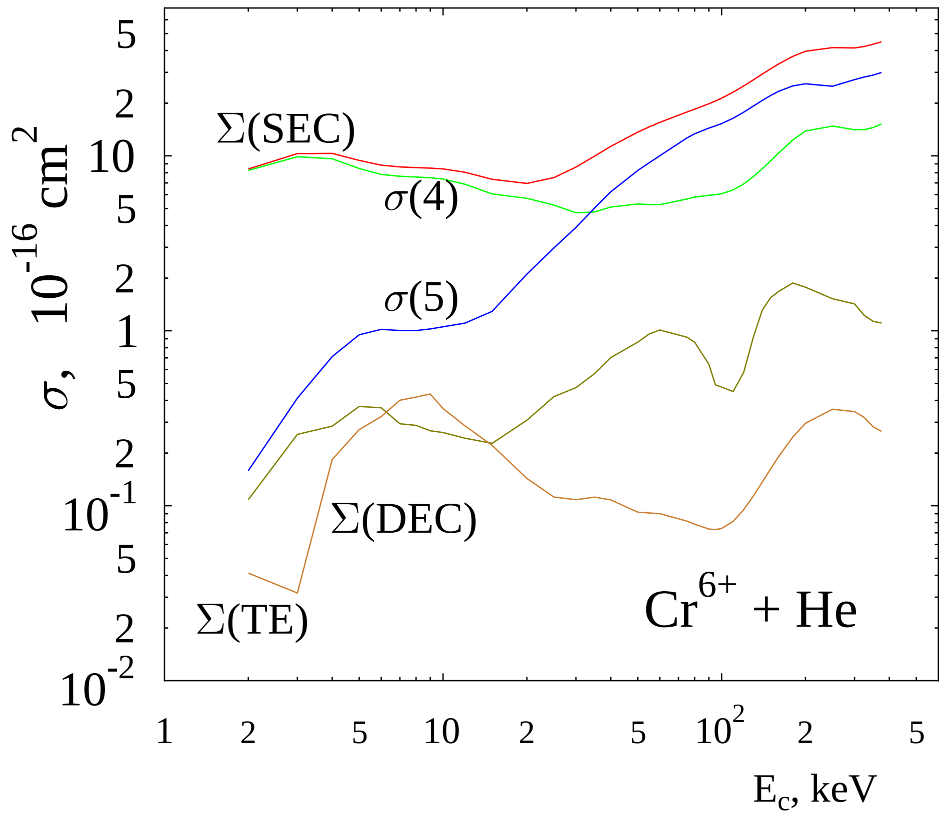

4.4. Fe^{8+} – He collision

Cross sections for SEC, DEC and TE channels were calculated [3] for the reactions

$$Fe^{8+}(3p^6) + He(1s^2) \rightarrow \begin{cases} Fe^{7+}(3p^6 nl) + He^+(1s) & (SEC) \quad (n = 4 - 7) \\ Fe^{6+}(3p^6 nl n'l') + He^{2+} & (DEC) \quad (n = 4, n' = 4, 5) \\ Fe^{7+}(3p^6 4f) + He^+(2l)\ ), & (TE) \end{cases} \quad (4)$$

The eight two-electron quasimolecular states for reactions (4) are shown in Fig. 7.

Figure 7: The energies $E_i(R)$ of the two-electron states $\phi_i(\psi_j, \psi_{j'})$ of the (Fe^{8+}+He) quasimolecule:
a) the entrance channel (red curve) – $\phi_1(4f\sigma', 4f\sigma')$;
b) the channels of SEC into 4f-, 5g-, 6h-, 7i- states of Fe^{7+}(nl) ions – $\phi_2(4f\sigma, 5g\sigma)$, $\phi_3(4f\sigma, 6h\sigma)$, $\phi_4(4f\sigma, 7i\sigma)$, $\phi_5(4f\sigma, 9k\sigma)$;
c) the channels of DEC into $4f^2$- and 4f5g-states of Fe^{6+} ions – $\phi_6(5g\sigma', 5g\sigma')$, $\phi_7(5g\sigma^*, 6h\sigma^*)$;
d) the channel of TE (SEC into 4f-state of Fe^{7+} ion with 1s$\longrightarrow$ $2p_0$ excitation of He atom) – $\phi_8(5g\sigma, 8j\sigma)$.

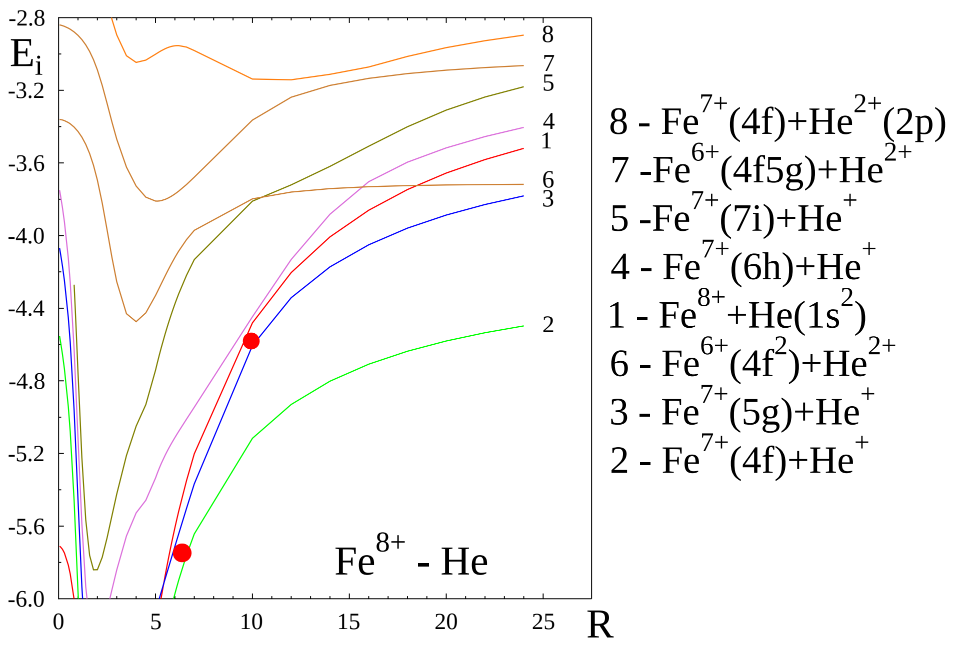

The calculated cross sections for Fe^{6+} + He($1s^2$) in the energy range from 2 to 400 keV are shown in Fig. 8. The maximum value of the total SEC cross section obtained for Fe^{8+}– He collision is equal to 1.3×10^{-14} cm^2 at $E_c \simeq$ 400 keV; the value of DEC cross section is less than 1.3×10^{-17} cm^2.

Figure 8:
The calculated cross sections as a function of the impurity ion energy E_c for Fe^{8+} + He collision: Σ(SEC) – the total cross section of SEC +TE; $\sigma(n)$ – cross sections of SEC into n-shells with n=4–7 of Fe^{7+} ions, σ(TE)– TE cross section; Σ(DEC) – DEC cross section.

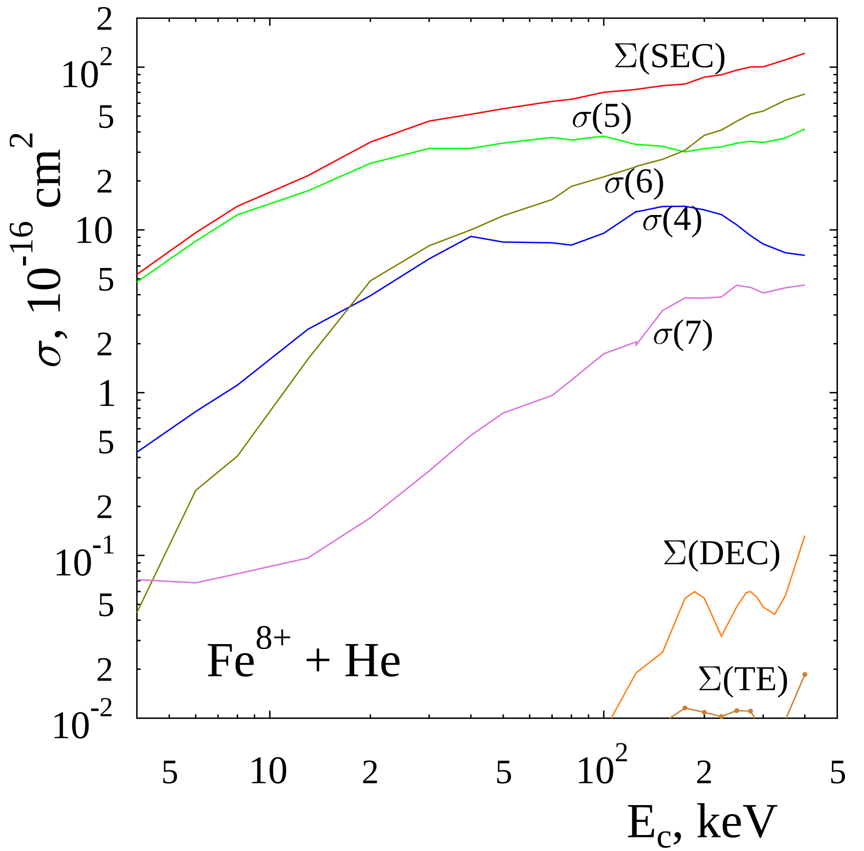

4.5. Mo^{6+} – He collision

Cross sections for SEC, DEC and TE channels were calculated [11] for the reactions

$$\mathrm{Mo}^{6+}(4p^6) + \mathrm{He}(1s^2) \rightarrow \begin{cases} \mathrm{Mo}^{5+}(4p^6 nl) + \mathrm{He}^{+}(1s) & (\mathrm{SEC}) \quad (n = 4-6) \\ \mathrm{Mo}^{5+}(4p^6 4d) + \mathrm{He}^{+}(2l) & (\mathrm{TE}) \\ \mathrm{Mo}^{4+}(4p^6 4dn'l') + \mathrm{He}^{2+} & (\mathrm{DEC}) \quad (n' = 4-6). \end{cases} \quad (5)$$

Figure 9: The energies $E_i(R)$ of the fourteen two-electron quasimolecular states $\phi_i(\psi_j, \psi_{j'})$:
a) the entrance channel (red curve) – $\phi_1(4f\sigma', 4f\sigma')$;
b) the channels of SEC into nℓ-states of ions $Mo^{5+}(nl)$ with n=4-6 – $\phi_2(4f\sigma, 5g\sigma)$; $\phi_3(4f\sigma, 5d\sigma)$, $\phi_4(4f\sigma, 5f\sigma)$, $\phi_5(4f\sigma, 6h\sigma)$, $\phi_6(4f\sigma, 6f\sigma)$, $\phi_7(4f\sigma, 7h\sigma)$, $\phi_8(4f\sigma, 8j\sigma)$;
c) the channels of DEC into 4d4f-, 4d5d-, 4f5f- and 4f5g-states of Mo^{4+} ions – $\phi_{11}(4d\sigma', 5d\sigma')$, $\phi_{12}(4d\sigma', 5g\sigma')$, $\phi_{13}(4d\sigma', 5f\sigma')$, $\phi_{14}(4d\sigma', 6h\sigma')$;
d) the channel of TE (SEC into 4d-state of Mo^{5+} ion with the 1s$\rightarrow$ $2l$ excitation of He atom) – $\phi_9(4d\sigma, 6g\sigma)$, $\phi_{10}(4d\sigma, 7i\sigma)$.

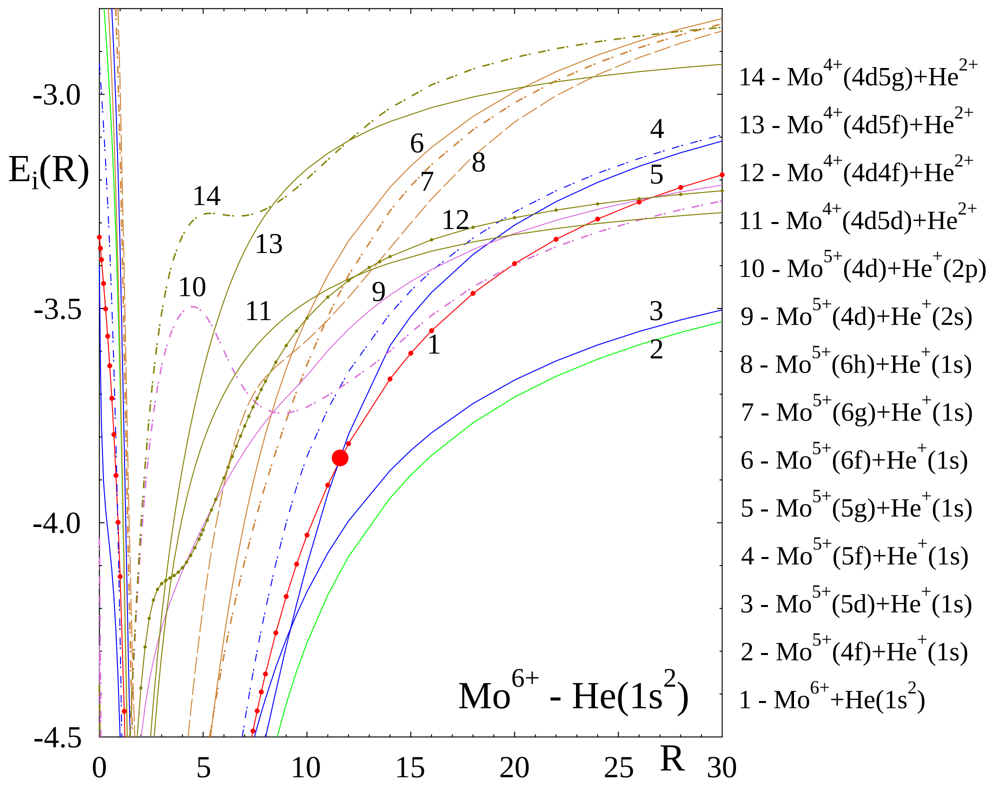

The SEC and DEC cross sections in collisions between Mo^{6+} ions with energies range of 5 – 400 keV and helium atoms are presented in Fig. 10. SEC into 5g-state of Mo^{5+} ion dominates at all energies. The maximum value of the total SEC cross section was obtained to be equal 1.1×10^{-14} cm^2 at the collision energy $\sim$ 175 keV; DEC cross section was obtained to be less than 1.6×10^{-17} cm^2.

Figure 10: The calculated cross sections as a function of the impurity ion energy E_c for Mo^{6+}+He collision: $\Sigma(\mathrm{SEC})$ $(\sigma(4)+\sigma(5)+\sigma(6)+\sigma(\mathrm{TE}))$ – the total SEC+TE cross section, $\sigma(n)$ – SEC cross sections into n-shells of Ni^{5+} ions with n=4–6, $\Sigma(\mathrm{TE})$ – TE cross section; $\Sigma(\mathrm{DEC})$ – DEC cross section.

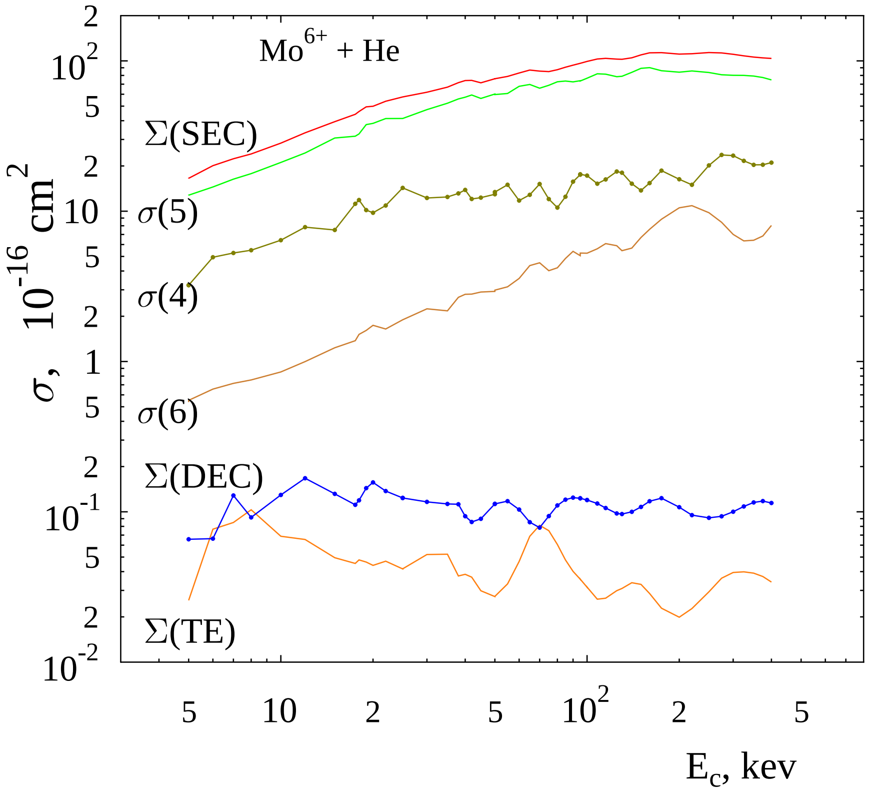

4.6. Ni^{6+} – He collision

Cross sections for SEC channels were calculated [12] for the reactions

$$\mathrm{Ni}^{6+}(3d^4) + \mathrm{He}(1s^2) \rightarrow \left\{ \; \mathrm{Ni}^{5+}(3d^4 nl) + \mathrm{He}^{+}(1s) \quad (\mathrm{SEC}) \quad (n = 4-7). \right. \qquad (6)$$

The eleven two-electron quasimolecular states for reactions (6) are shown in Fig. 11.

Figure 11: The energies $E_i(R)$ of the two-electron states $\phi_i(\psi_j, \psi_{j'})$ of the (Ni^{6+} + He^{2+}) quasimolecule:
a) the entrance channel (red curve) – $\phi_1(4f\sigma', 4f\sigma')$;
b) the channels of SEC into nℓ-states of ions $Ni^{5+}(nl)$ with n=4-7 –
$\phi_9(4f\sigma, 4d\sigma)$, $\phi_2(4f\sigma, 5g\sigma)$,
$\phi_{10}(4f\sigma, 4f\pi)$;
$\phi_3(4f\sigma, 5d\sigma)$, $\phi_4(4f\sigma, 6g\sigma^*)$,
$\phi_5(4f\sigma, 6h\sigma)$;
$\phi_6(4f\sigma, 6f\sigma)$, $\phi_7(4f\sigma, 7h\sigma)$,
$\phi_8(4f\sigma, 8j\sigma)$, $\phi_{11}(4f\sigma, 9k\sigma)$.

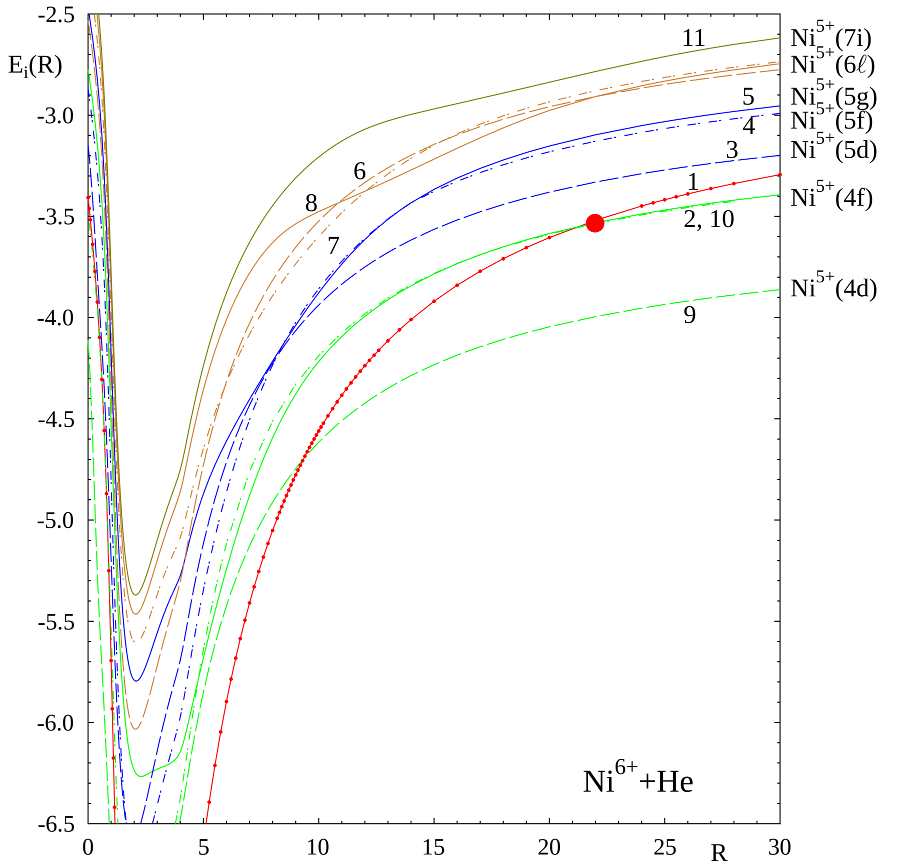

The calculated total and partial SEC cross sections for Ni^{6+} + He collision in the energy range from 5 keV to 500 keV are shown in Fig. 12. It is clearly seen that SEC into $4\mathrm{f}_0$ and $4\mathrm{f}_{\pm1}$ states of the Ni^{5+} ions dominates in overall range of collision energies. The maximum value of the total SEC cross section was obtained to be equal 4.6×10^{-16} cm^2 at the collision energy 500 keV.

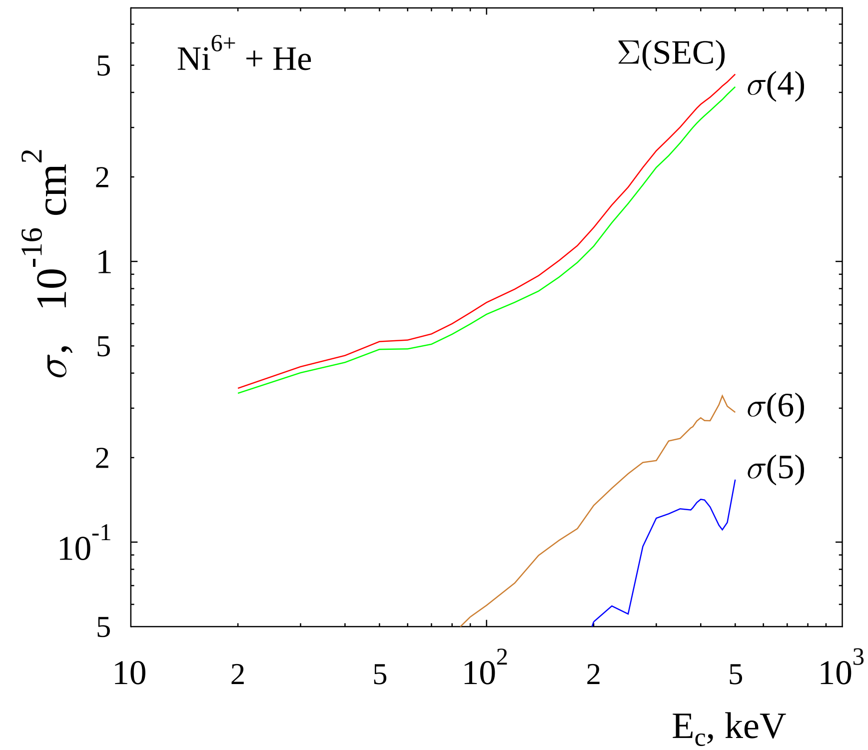

Figure 12: The calculated cross sections as a function of the impurity ion energy E_c for Ni^{6+}+He collision: $\Sigma(\mathrm{SEC})$ – the total SEC cross section, $\sigma(n)$ – the SEC cross sections into n-shells of Ni^{5+} ions with n=4-6.

4.7. Cu^{6+} – He collision

Cross sections for SEC, DEC and TE channels were calculated [13] for the reactions

$$Cu^{6+}(3d^5) + He(1s^2) \rightarrow \left\{ \; Cu^{5+}(3d^5 nl) + He^{+}(1s) \quad (SEC) \quad (n = 4 - 7). \right. \qquad (7)$$

The eleven two-electron quasimolecular states for reactions (7) are shown in Figure 13.

Figure 13: The energies $E_i(R)$ of the two-electron states $\phi_i(\psi_j, \psi_{j'})$ of the (Cu^{6+}+He) quasimolecule:

a) the entrance channel (red curve) – $\phi_1(4f\sigma', 4f\sigma')$;

b) the channels of SEC into $n\ell$-states with n=4-7 of Cu^{5+} ions –

$\phi_9(4f\sigma, 4d\sigma)$, $\phi_2(4f\sigma, 5g\sigma)$,

$\phi_{10}(4f\sigma, 4f\pi)$;

$\phi_3(4f\sigma, 5d\sigma)$, $\phi_4(4f\sigma, 6g\sigma)$,

$\phi_5(4f\sigma, 6h\sigma)$;

$\phi_6(4f\sigma, 6f\sigma)$, $\phi_7(4f\sigma, 7h\sigma)$,

$\phi_8(4f\sigma, 8j\sigma)$;

$\phi_{11}(4f\sigma, 9k\sigma)$.

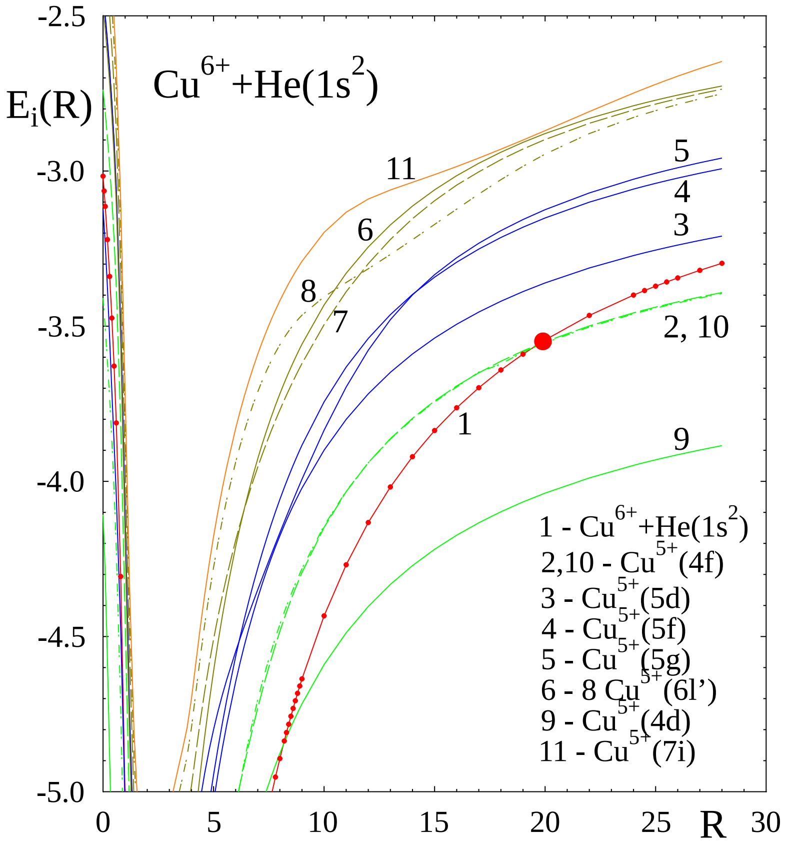

The calculated cross sections as a function of the Cu^{6+} ion energy 10 - 500 keV are shown in Figure 14. The maximum value of the total SEC cross section was obtained to be equal 67×10^{-16} cm^2 at the collision energy 500 keV. The channels of SEC into 4f states of the Cu^{5+} ions make the main contribution.

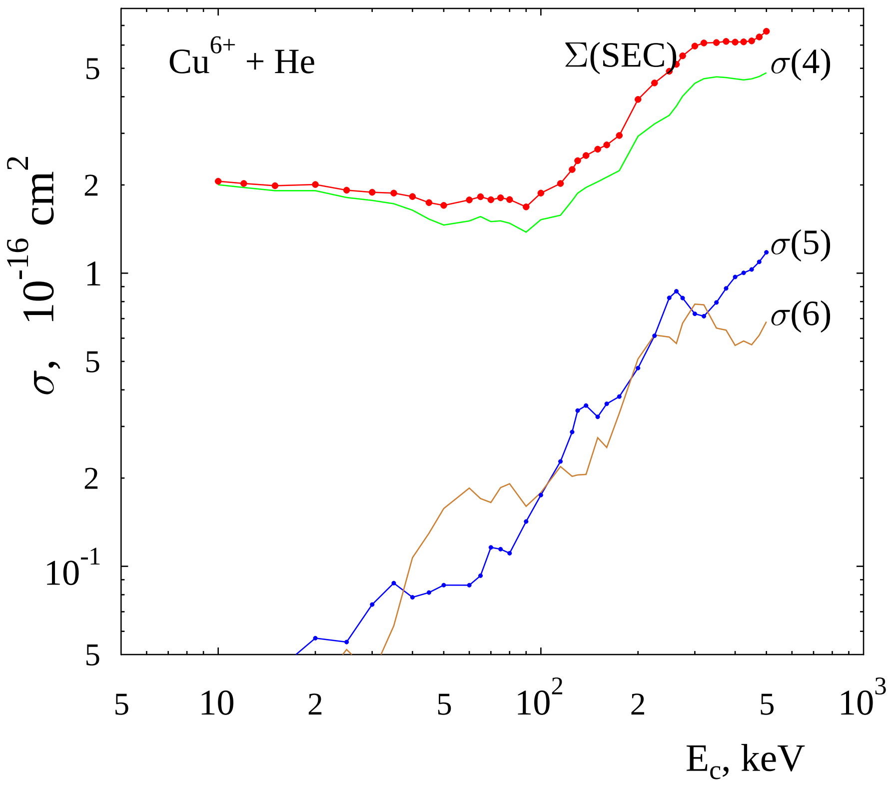

Figure 14: The calculated cross sections as a function of the impurity ion energy E_c for $Cu^{6+} + He(1s^2)$ collision: $\sigma(n)$ - SEC cross sections into n shell of Cu^{5+} ions, Σ(SEC) - the total SEC cross section.

4.8. W^{6+} – He collision

Cross sections for SEC channels were calculated [10] for the reactions

$$W^{6+}(5p^6) + He(1s^2) \rightarrow \Big\{ \; W^{5+}(5p^6 nl) + He^+(1s) \quad (SEC) \quad (n = 5-7). \qquad (8)$$

The nine two-electron quasimolecular states for reactions (8) are shown in Fig. 15.

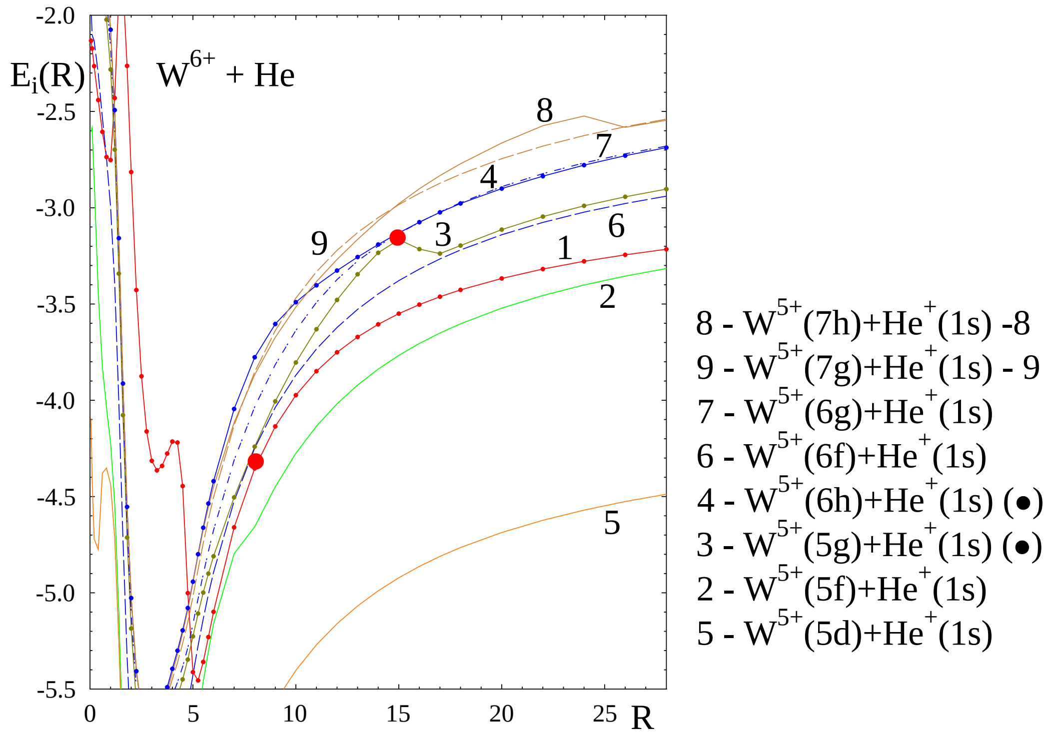

Figure 15: The energies $E_i(R)$ of the two-electron states $\phi_i(\psi_j, \psi_{j'})$ of the (W^{6+}+He) quasimolecule:

a) entrance channel (red curve) – ϕ_1=5gσ^2;

b) the channels of SEC into nℓ-states of ions $W^{5+}(nl)$ with n=5-7 –

ϕ_2=[5gσ,5fσ], ϕ_3=[5gσ,7iσ^*],

ϕ_5=[5gσ,5dσ];

ϕ_6=[5gσ,6fσ], ϕ_4=[5gσ,8jσ],

ϕ_7=[5gσ,7hσ];

ϕ_8=[5gσ,8iσ], ϕ_9=[5gσ,8hσ].

The calculated total and partial SEC cross sections for collision of the W^{6+} ions with energies of 20 – 800 keV with helium atoms are shown in Fig.16. The channels of the electron capture into 5g and 6h states of W^{5+} ions make the main contribution at the collision energy of 500 keV. The maximum value of the total SEC cross section at this energy was obtained to be equal 6.7×10^{-15} cm^2.

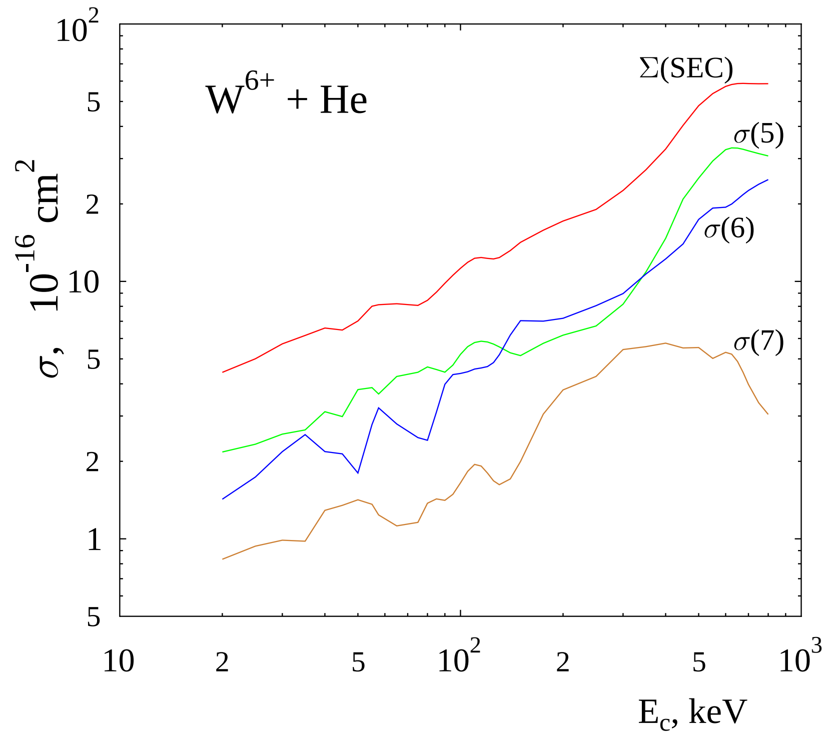

Figure 16: The calculated cross sections as a function of the impurity ion energy E_c for W^{6+}+He collision: $\Sigma(\mathrm{SEC})$ - the total single electron transfer cross section, $\sigma(5)$, $\sigma(6)$, and $\sigma(7)$ – SEC cross sections into n-shells of the W^{5+} ion with n=5-7.

4.9. Results obtained

Data on the partial and total cross sections for electron transfer, transfer excitation, and excitation in collisions of multiply charged impurity ions with the helium atoms were obtained for the first time in the energy range of ions 2 ÷ 800 keV. The calculated total cross sections of the single-electron transfer as a function of the impurity ion energy E_c for collisions $A^{q+} + He(1s^2)$ are shown in Fig. 17.

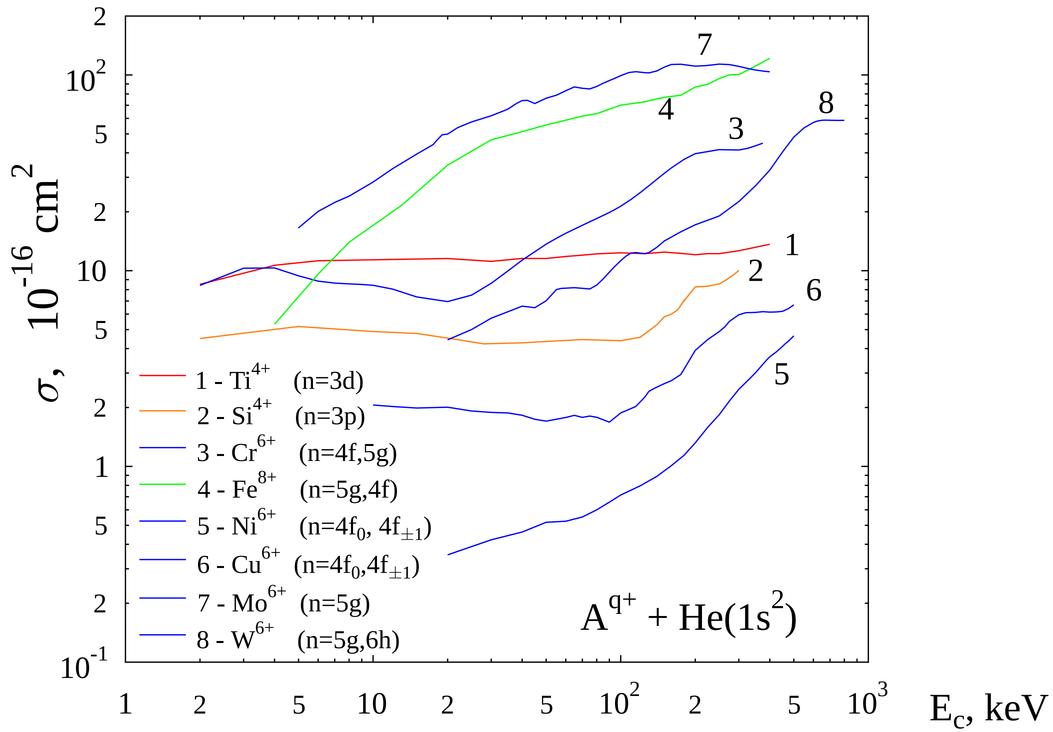

Destruction of ground and especially excited states of abundant neutral atomic and molecular hydrogen and the He atoms by SEC and DEC in their collisions with metallic impurity ions are the most important processes in the edge plasmas.

5. Theoretical study of the single-electron transfer and excitation processes in collisions of Ti^{4+}, Cr^{6+}, and Fe^{8+} with helium atoms in the metastable state

The electron transfer and excitation in collisions between impurities and helium atoms in excited states from atomic beams used for edge and central plasma diagnostics could be important in the level population. Atomic and ion species in metastable excited states have significant effects on the kinetics of partially ionized edge and divertor plasmas. The most important of the collision processes involving metastables and plasma impurity ions are those leading to the excitation of metastables or the electron capture. Recently within IAEA projects, a serious effort was made by theorists to determine the relevant cross sections involving light impurities.

The state selective and total cross sections for electron capture, excitation and ionization processes in slow collisions of H(2s) and He^{+}(2s) with light bare ions (Z=1–5) were calculated by R. Janev et al [19] by using the hidden crossing method. Electron transfer and excitation cross sections have been determined by W. Fritsch and H. Tawara [22] for Be^{4+}– He collision with an initially excited He(1s2s) 2 ^{1}S target using the close-coupling equation method with a one-electron AO expansion.

The classical trajectory Monte Carlo (CTMC) calculations of state selective SEC and EXC cross sections for collisions between excited helium and bare light ions (Z=3–6,8) were performed in paper [21].

We carried out [4, 5] the close coupling calculation of the single electron capture and excitation cross sections for slow collisions:

$$\mathrm{A}^{6+}(3p^6) + \mathrm{He}(1s2s) \to \begin{cases} \mathrm{A}^{5+}(3p^6 n'l') + \mathrm{He}^{+}(1s) & \mathrm{(SEC)} \\ \mathrm{A}^{6+}(3p^6) + \mathrm{He}(1sn'l')\ (n'=2,3), & \mathrm{(EXC)} \quad (\mathrm{A} = \mathrm{Ti}, \mathrm{Cr}, \mathrm{Fe}). \end{cases}$$

The cross sections of the processes were calculated by the close-coupling method with the basis of seventeen one-electron states for Ti^{4+}+He(1s2s) collision and ten states for Cr^{6+}, Fe^{8+}+He(1s2s) collisions.
The calculated one-electron screened diatomic molecular orbital (SDMO) correlation diagrams [12] for quasimolecules (Ti^{4+}+He^{+}(1s))e, (Cr^{6+}+He^{+}(1s))e, and (Fe^{8+}+He^{+}(1s))e are shown in Fig. 18 – 20.

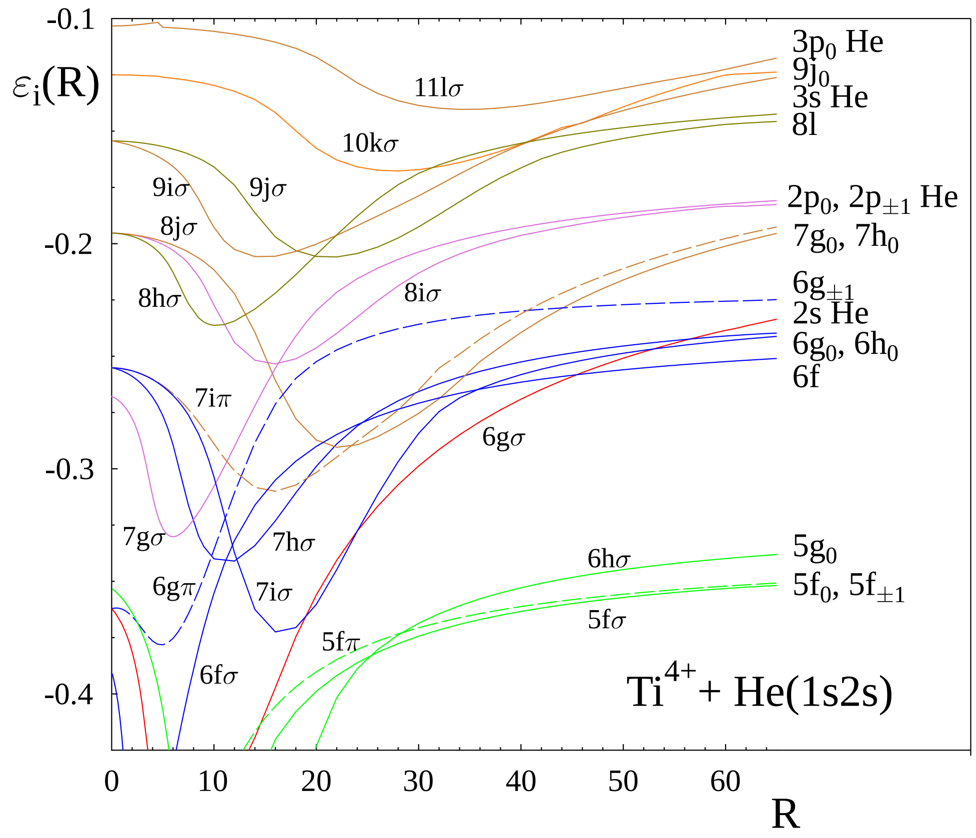

Figure 18: The energies ε_j(R) of SDMO $\psi_j(r;\mathrm{R})$ of the (Ti^{4+}+ He^{+}(1s))**e** quasimolecule and their atomic limits at R $\longrightarrow \infty$:

a) the entrance channel (red curve) – He(2s) state (6gσ);

b) the channels of SEC into nℓ-states of Ti^{3+} ions: n=5 – $5f_0$-, $5f_{\pm1}$-, $5g_0$-states (5fσ, 5fπ, 6hσ);

n=6 – $6f_0$-, $6g_0$-, $6g_{\pm1}$-, $6h_0$-states (6fσ, 7hσ, 6gπ, 7iσ);

n=7 – $7g_0$-, $7h_0$-states (7gσ, 8iσ);

n=8 – $8h_0$-, $8i_0$-states (8hσ, 9jσ);

n=9 – $9j_0$-state (10kσ);

c) the channels of the 2s$\longrightarrow$ nℓ excitation of He(1s2s) atoms: nℓ=$2p_0$, $2p_{\pm1}$ (8jσ, 7iπ), and nℓ=3s, $3p_0$ (9iσ, 11lσ).

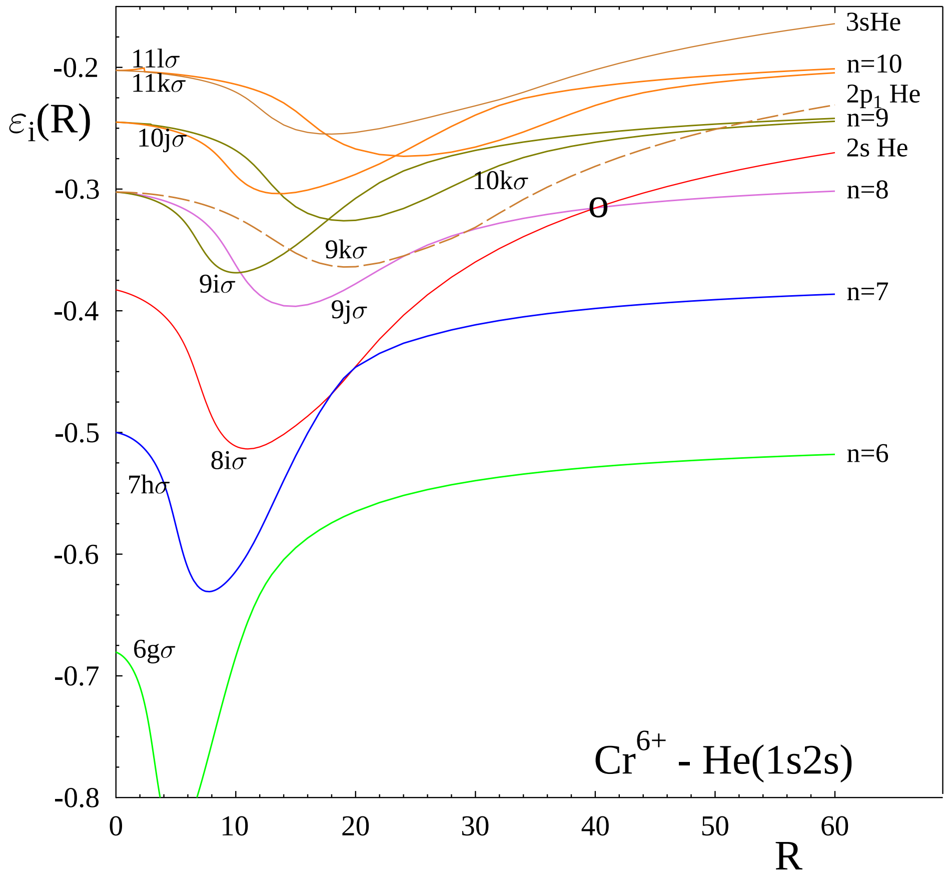

Figure 19: The energies ε_j(R) of SDMO $\psi_j(r;\mathrm{R})$ of the (Cr^{6+}+ He^{+}(1s))**e** quasimolecule and their atomic limits at R $\to\infty$: a) the entrance channel (red curve) – He(2s) state (8iσ); b) the channels of SEC into nℓ-states of Cr^{5+} ions: n=6 – 6g$_0$-state (ψ_2=6gσ), n=7 – 7h$_0$-state (ψ_3=7hσ), n=8 – 8i$_0$-states (ψ_4=9jσ), n=9 – 9i$_0$-, 9j$_0$-states – (ψ_5=9iσ, ψ_6=10kσ), n=10 –10j$_0$-, 10k$_0$-states (ψ_7=10jσ, ψ_8=11$\ell\sigma$); c) the channels of electron 2s$\longrightarrow$ nℓ excitation of He(1s2s) atoms: nℓ=3s (ψ_9=11kσ), 2$p_{\pm1}$ (ψ_{10}=9kπ).

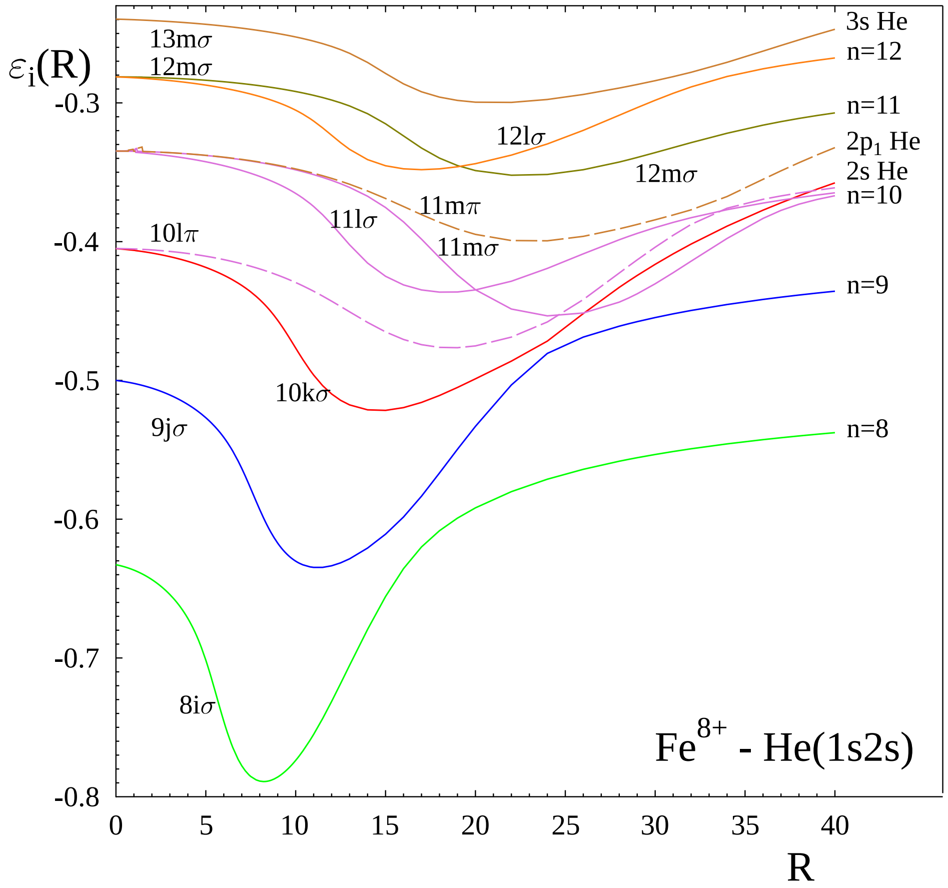

Figure 20: The energies ε_j(R) of SDMO $\psi_j(r;\mathrm{R})$ of the (Fe^{8+}+ He^{+}(1s))**e** quasimolecule and their atomic limits at R $\to\infty$: a) the entrance channel (red curve) – He(2s) state (10kσ); b) the channels of SEC into nℓ-states of Fe^{7+} ions: n=8 – 8i_0-state (ψ_2=8iσ), n=9 – 9j_0-state (ψ_3=9jσ), n=10 – 10k_0-, 10ℓ_0-, 10$\ell_{\pm1}$ -states (ψ_4=11$\ell\sigma$, ψ_7=11mσ, ψ_8=10$\ell\pi$), n=11 – 11ℓ_0- state (ψ_5=12mσ), n=12 – 12ℓ_0-state (ψ_{10}=12$\ell\sigma$); c) the channels of electron 2s$\to$ nℓ excitation of He(1s2s) atoms: nℓ= 3s (ψ_6=13mσ), $2p_{\pm1}$ (ψ_9=11mπ).

Results obtained

The cross sections of SEC into nℓ-states of Ti^{3+} (n=5-8), Cr^{5+} (n=6-9), Fe^{8+} (n=8-11) and of the electron He(2s$\longrightarrow$3ℓ) excitation in collisions of the excited helium atoms He(1s2s) and the Ti^{4+} ions were obtained in the range of the ion energy E_c 5 –300 keV. The data are shown in graphical form in Figs. 21–23 and 27. The maximum values of the total electron transfer and excitation cross sections were obtained to be equal 2.05×10^{-14} cm^2 and 7.70×10^{-16} cm^2 (at E_c=300 keV) for Ti^{4+} + He collision, 2.32×10^{-14} cm^2 and 2.00×10^{-15} cm^2 (at E_c=400 keV) for Cr^{6+}+ He collision, and 3.40×10^{-14} cm^2 and 9.54×10^{-15} cm^2 (at E_c=400 keV) for Fe^{8+}+ He collision, respectively.

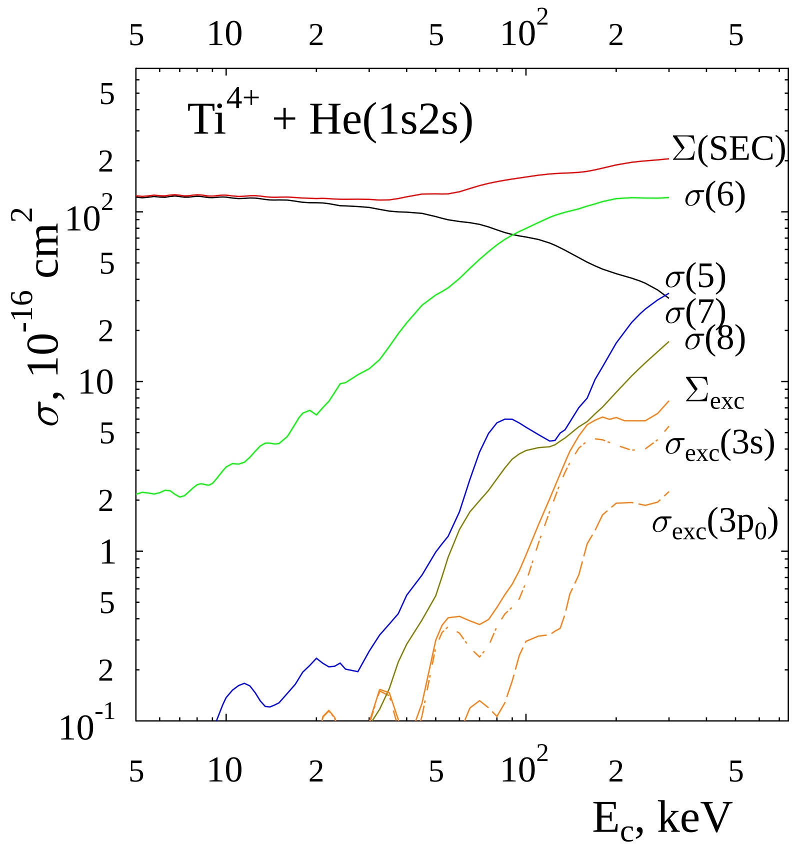

Figure 21: The calculated cross sections as a function of the impurity ion energy E_c for the Ti^{4+}+He(1s2s) collision: Σ(SEC) – the total SEC cross section, $\sigma(n)$ – SEC cross sections into n-shells with n=6–8 of the Ti^{3+} ions; Σ(EXC) and $\sigma_{exc}(3\ell)$ – the total and partial cross sections of the electron 2s$\longrightarrow$3ℓ excitation in He atoms .

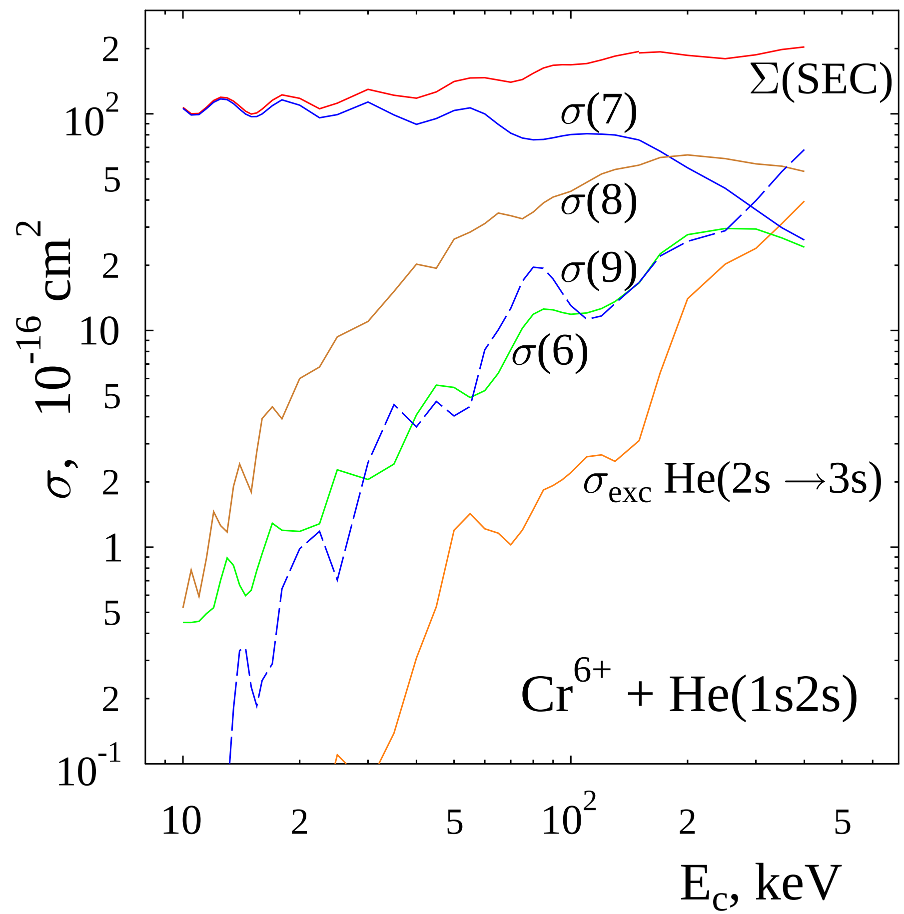

Figure 23: The calculated cross sections as a function of the impurity ion energy E_c for the Cr^{6+}+He(1s2s) collisions: Σ(SEC) – the total SEC cross section; $\sigma(n)$ – SEC cross sections into n-shells with n=6-9 of the Cr^{5+} ions; $\sigma_{exc}(3s)$ – the cross section of electron 2s⟶3s excitation in He atoms.

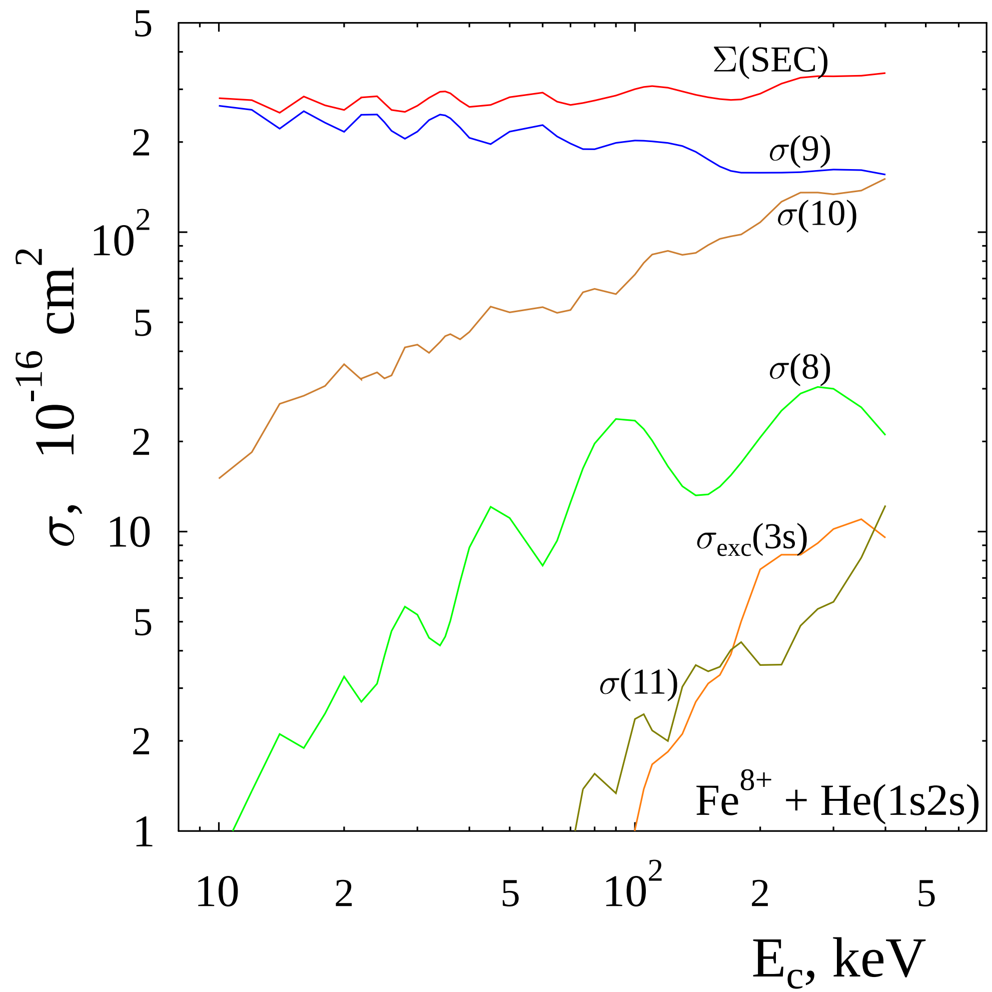

Figure 24: The calculated cross sections as a function of the impurity ion energy E_c for Fe^{8+}+He(1s2s) collision: Σ(SEC) – the total SEC cross section ; $\sigma(n)$ – SEC cross sections into n-shells with n=8-11; $\sigma_{exc}(3s)$ – the cross section of electron He(2s⟶3s) excitation.

Calculated n-distribution of the electron transfer cross section for the Ti^{4+}, Cr^{6+}, Fe^{8+}– He(1s2s) collisions is shown in Figs. 24–26. In Fig. 24 we compare the calculated n-distribution in the Ti^{4+} – He(1s2s) collision at 240 keV (5 keV/u) with results by Fritsch and Tawara [20] for the Be^{4+} – He(1s2s) collisions. The agreement is only qualitative because we considered the Ti^{4+} ion with the Ar-like core but not the bare ion.

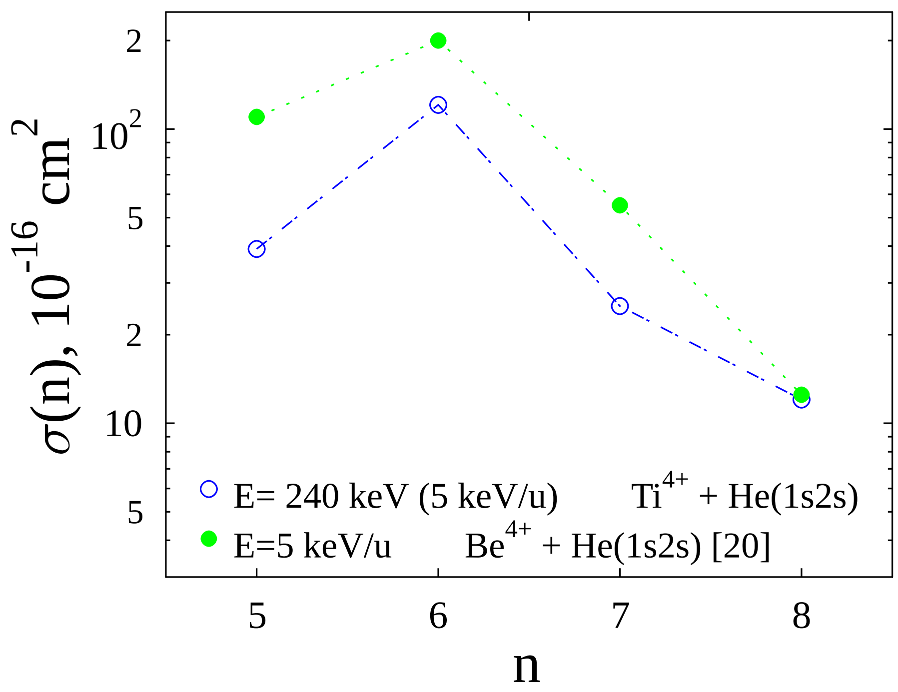

Figure 25: The n-distribution of SEC cross sections in the Ti^{4+}+ He(1s2s) collision from our calculation (○- blue curve) and in Be^{4+}+ He(1s2s) from [20] (● -green curve) at 5 keV/u.

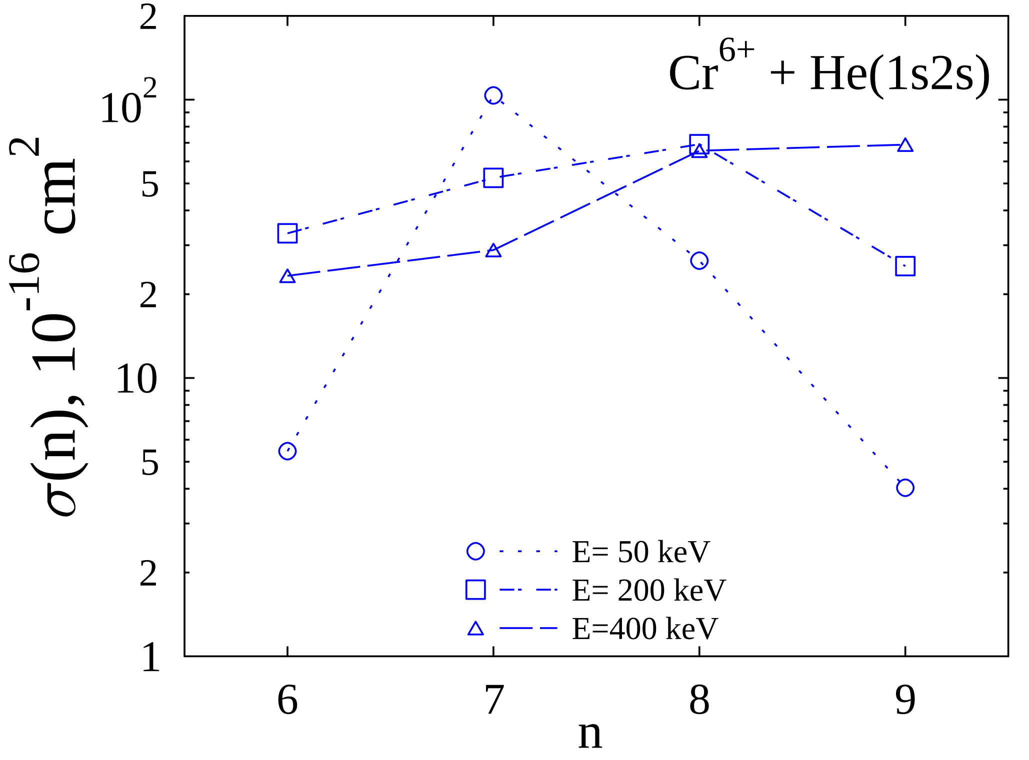

Figure 26: Calculated n-distribution of SEC cross sections in the Cr^{6+}+ He(1s2s) collision.

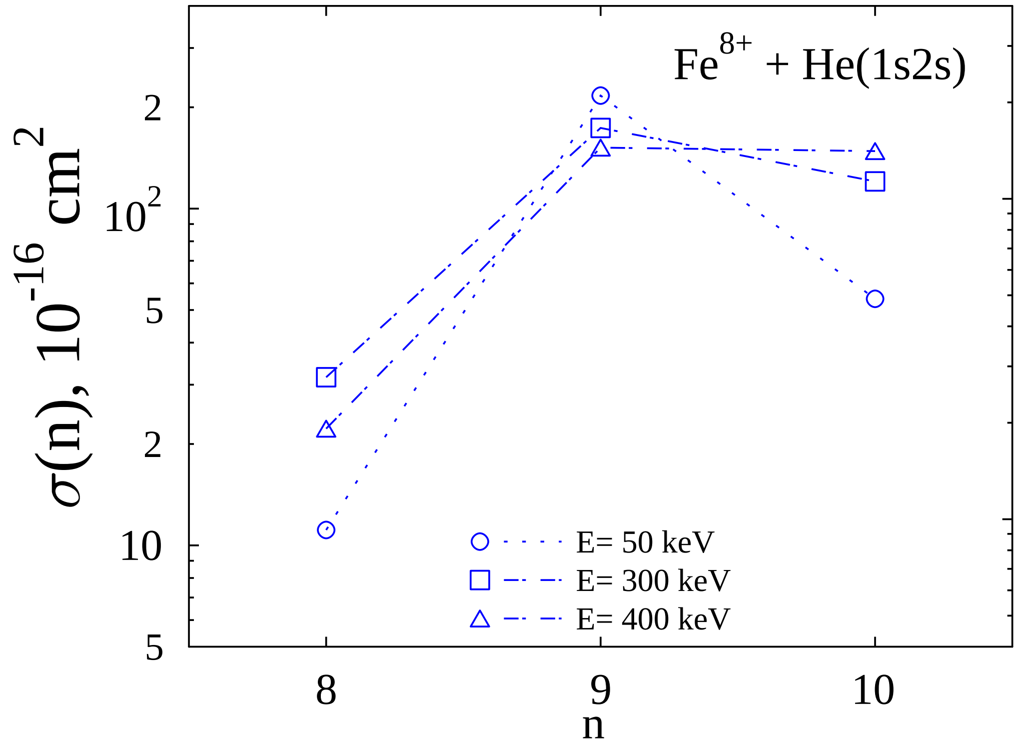

Figure 27: Calculated n-distribution of SEC cross sections in the Fe^{8+}+ He(1s2s) collision.

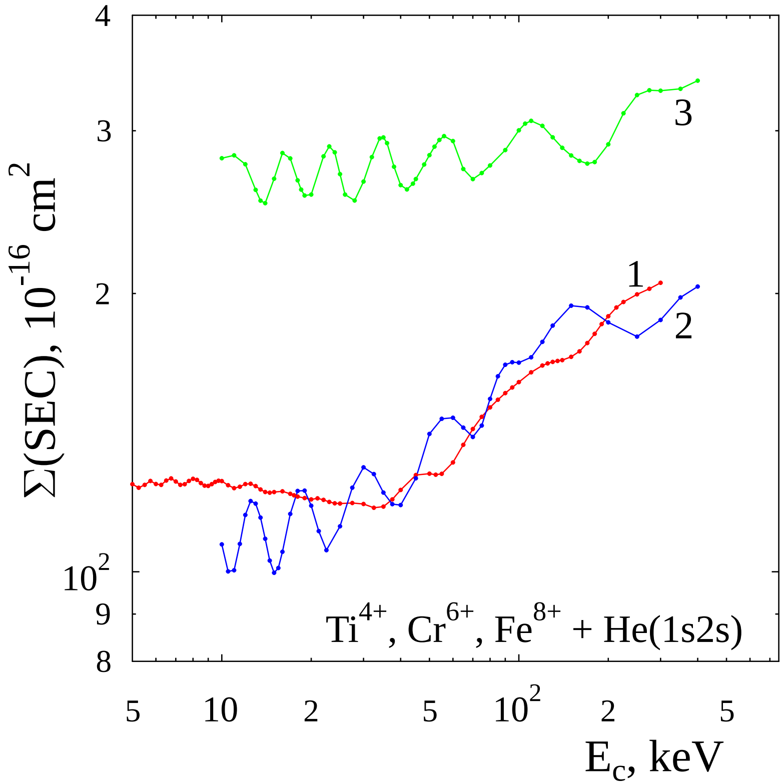

Figure 28: Calculated total cross sections of the single-electron transfer as a function of the impurity ion energy E_c for collisions: 1 – Ti^{4+}+ He(1s2s) 2 – Cr^{6+}+ He(1s2s), 3 – Fe^{8+}+ He(1s2s).

The charge transfer cross sections in the collisions of impurity ions with metastable helium atoms are of the order of magnitude larger than the corresponding cross sections for the ground-state helium. A small admixture of metastable helium in a neutral beam can hence considerable change spectra of charge-exchange spectroscopy.

6. Study of alpha particle neutralization through quasi-resonant double electron capture in slow collisions with C^{2+} and Ti^{2+} ions

Previously the key role of the alpha-particle neutralization reactions in cooling the edge plasmas was discussed by Tawara [22]. The reactions were due to DEC into metastable He^{o}(1s3l) state at collisions of alpha-particles with H_2 in low eV-energies. DEC cross sections in this collisions into the $He^{o}(1s^2)$ ground state were known to be small.

Slow collisions of alpha particles with the Be-like C^{2+} ions (four-electron quasimolecule) and the Ti^{2+} ions (two-electron quasimolecule) [14] were considered in our study.

$He^{2+} + C^{2+}(1s^2 2s^2)$

In slow ion-atom collisions, SEC reactions are generally dominant with only one exception – the collision system C^{4+}– He. DEC dominates over SEC at collision energies below 20 keV, according to Grandall [23] for collisions:

$$C^{4+}(1s^2) + He(1s^2) \rightarrow \qquad C^{2+}(1s^2 2s^2) + He^{2+}.$$

It is believed that DEC would dominate over SEC for the inverse ion-ion reaction $He^{2+} + C^{2+}(1s^2 2s^2)$. Calculations for this reaction were carried out using the close-coupling equation method with the basis of nine quasimolecular four-electron states. The results of our calculations for direct and inverse reactions were fully identical. It means that the same channels are responsible for the reactions.

Results of our calculation of the DEC cross section for direct reaction, using six four-electron quasimolecular states, are shown in Fig. 28. In the high velocity limit, there is agreement between theoretical results and experiment. It is clearly seen that at low energies, our results are in better agreement with experiment.

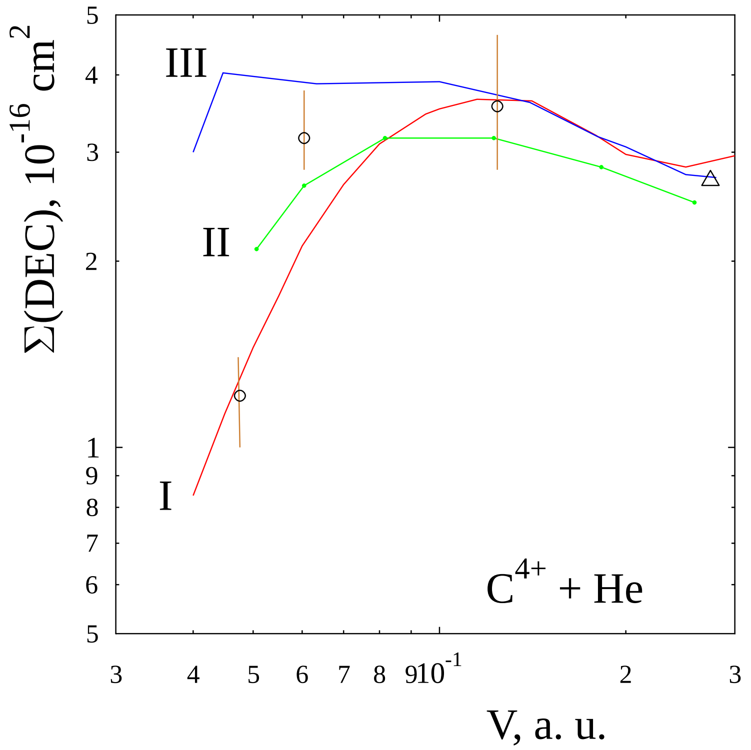

Figure 29: Total double-electron capture cross sections for the $C^{4+} + He \rightarrow C^{2+} + He^{2+}$ collision as a function of the relative velocity **V**. Theoretical results: I – present results; II – results by Kimura and Olson [24], III – results by Errea et al [25]. Experimental data: (o) data by Phaneuf and Grandall [26]; (Δ) data by Grandall [23].

$He^{2+} + Ti^{2+}(3d_0^2)$ collisions

The energy of seventeen two-electron quasimolecular states for the collisions are shown in Fig. 29.

Figure 29: The energies $E_i(R)$ of two-electron states $\phi_i(\psi_j, \psi_{j'})$ of the $(He^{2+}+Ti^{2+}(3d_0^2))$ quasimolecule: a) the entrance channel (● red) – $\phi_{14}(4f\sigma', 4f\sigma')$, b) channels of the DEC into $1s^2$, 1s2s, $1s2p_{\pm1}$, $1s3p_0$, and $1s3p_{\pm1}$ – $\phi_1(3d\sigma', 3d\sigma')$; $\phi_8(3d\sigma, 5f\sigma')$, $\phi_{10}(3d\sigma, 5g\pi')$, $\phi_9(3d\sigma, 8i\sigma')$, $\phi_{11}(3d\sigma, 7h\pi')$; c) channels of SEC into the 1s, 2s, and $2p_0$ states of the He^+ ions – $\phi_{12}(3d\sigma, 4f\sigma)$, $\phi_{16}(4f\sigma, 5f\sigma)$, $\phi_6(4f\sigma, 5g\sigma)$; d) the TE channels (the single-electron transfer into the 1s, 2p states of the He^+ ions with the $3d_0 \rightarrow 3d_{\pm1}$, $4f_0$, $5f_0$, and $5g_0$ excitation of the Ti^{3+} ion – $\phi_{13}(3d\sigma, 3d\pi)$, $\phi_3(3d\sigma, 6h\sigma)$, $\phi_4(3d\sigma, 6g\sigma)$, $\phi_5(3d\sigma, 7i\sigma)$, $\phi_{15}(3d\sigma, 4d\sigma)$, $\phi_7(4f\sigma, 4f\pi)$; d) channels of the $3d_0^2 \rightarrow 3p_0 3d_{\pm1}$, $3d_{\pm1}^2$ excitations of the Ti^{2+} ions – $\phi_2(4f\sigma', 3d\pi')$, $\phi_{17}(3d\pi', 3d\pi')$.

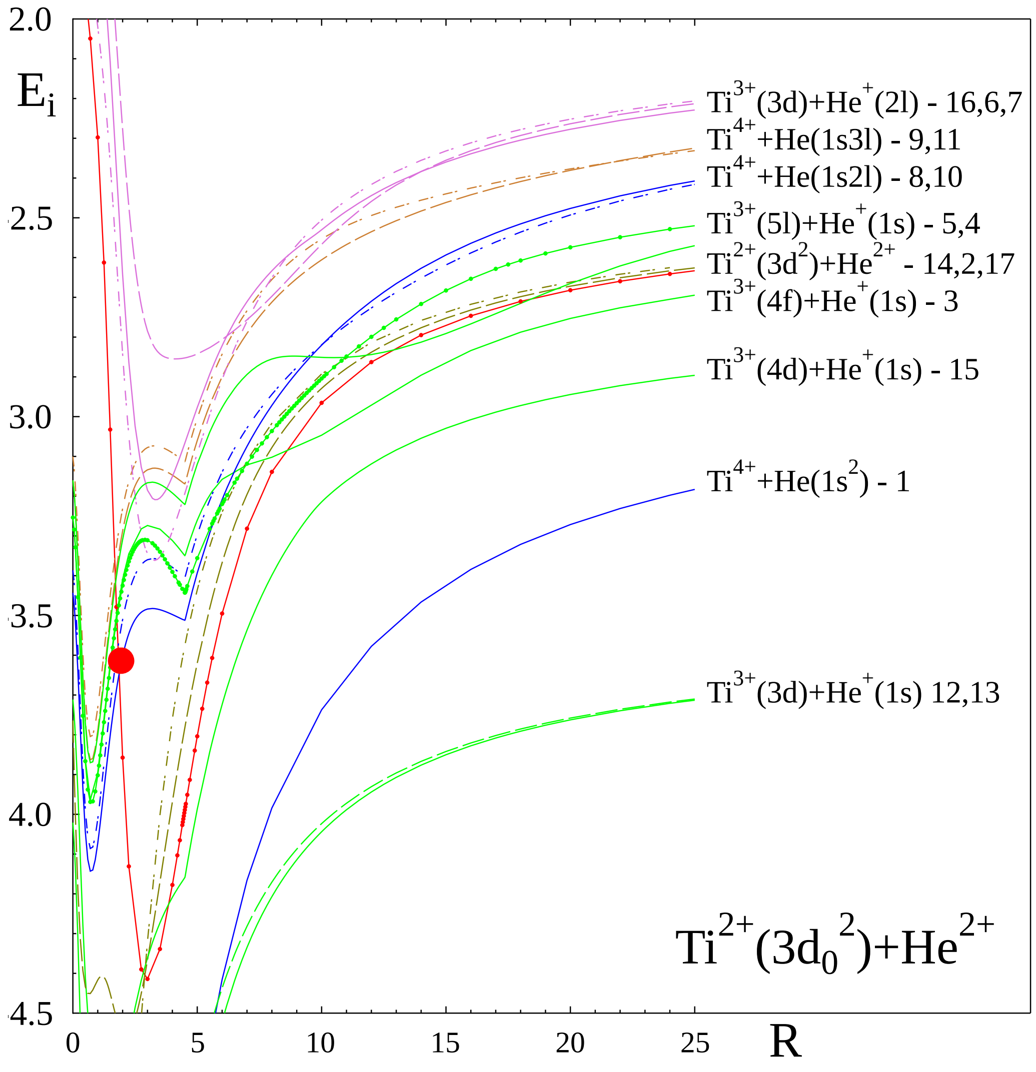

Results of our calculation of DEC cross section into the ground $\sigma(1s^2)$ and excited $\sigma(1s2s)+\sigma(1s2p_{\pm 1})$ and $\sigma(1s3p_0)+\sigma(1s3p_{\pm 1})$ states of the He atom are shown in Fig. 30. At low velocities, the capture into excited states dominates over the capture into the ground state of the He atom.

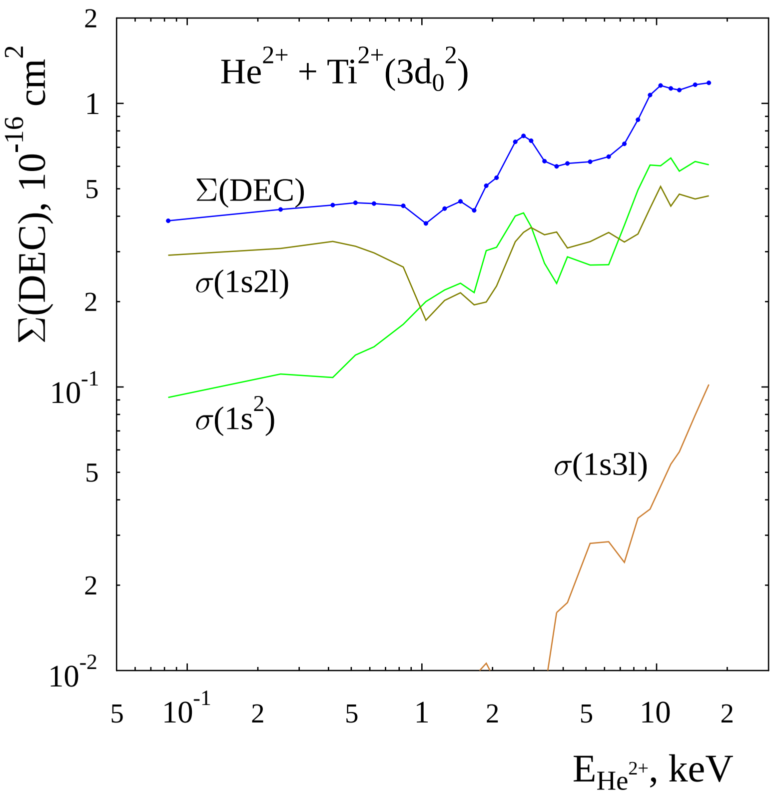

Figure 31: DEC cross sections for the $He^{2+}+Ti^{2+}(3d_0^2)$ collision as a function of the alpha particle energy: $\Sigma(\mathrm{DEC})$ – the total cross section, $\sigma(1s^2)$, $\sigma(1s2l)$, and $\sigma(1s3l)$ – the partial cross sections.

In fig. 3,1 the comparison between the cross sections of alpha particle neutralization obtained from the calculation for the direct reaction (DEC by the Ti^{4+} ion from the He atom) and for inverse reactions. In the high relative velocity limit (V$>$ 0.2 a.u.), there is qualitative agreement between the results.

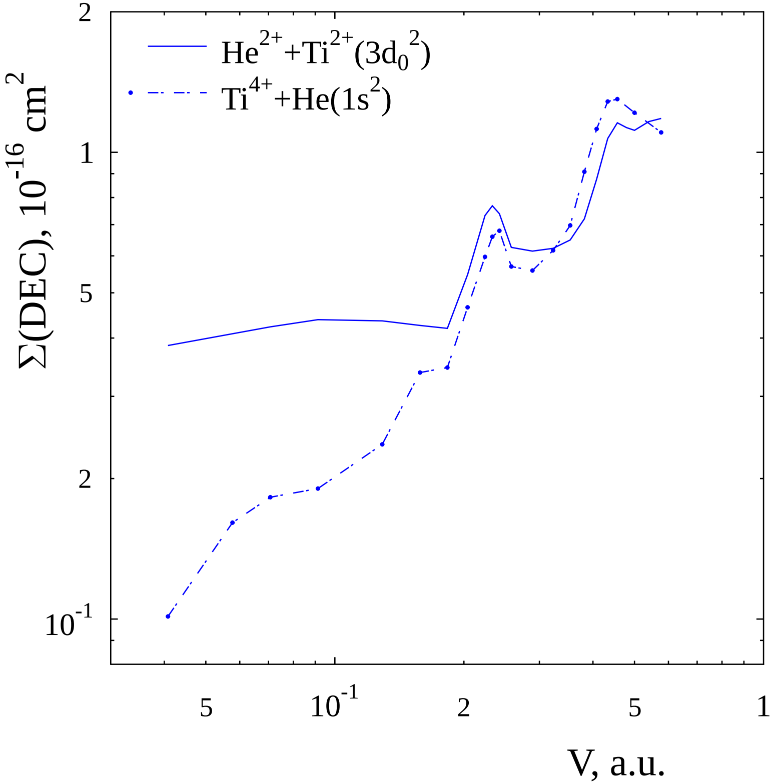

Figure 32: The alpha particle cross sections for direct the Ti^{4+} + He$(1s^2)$ (5) and inverse He^{2+}+Ti^{2+}$(3d_0^2)$ (4) reactions as a function of the relative velocity **V**.

7. Electron capture and excitation processes in collisions of alpha particles with Be-like oxygen ions – He^{2+} + $O^{4+}(1s^22s^2)$

The cross sections for SEC, TE and excitation were calculated with the basis of thirteen quasimolecular four-electron states in the energy range of the incident He^{2+} ions from 0.2 to 2 MeV for all exit channels from Table I.

Table I. Entrance, SEC, TE, single-electron excitation (SE EXC) and double-electron excitation (DE EXC) channels. Energies of resonance defects ΔE_p are obtained from atomic calculations.

channel	Φ_p	atomic limit at R $\rightarrow \infty$	ΔE_p (a.u.)
DE EXC	Φ_9	$He^{2+} + O^{4+}(1s^22p4f)$	ΔE_9=3.84
	Φ_7	$He^{2+} + O^{4+}(1s^22p3d)$	ΔE_7=3.19
	Φ_3	$He^{2+} + O^{4+}(1s^22p^2)$	ΔE_3=0.96
SE EXC	Φ_8	$He^{2+} + O^{4+}(1s^22s4f)$	ΔE_8=3.41
	Φ_6	$He^{2+} + O^{4+}(1s^22s3d)$	ΔE_6=2.75
	Φ_2	$He^{2+} + O^{4+}(1s^22s2p)$	ΔE_2=0.48
TE	Φ_{12}, Φ_{13}	$He^+(2l) + O^{5+}(1s^22p)$	$\Delta E_{12,13}$=3.97
	Φ_5	$He^+(1s) + O^{5+}(1s^22p)$	ΔE_5=2.47
SEC	Φ_{10}, Φ_{11}	$He^+(2l) + O^{5+}(1s^22s)$	$\Delta E_{10,11}$=3.59
	Φ_4	$He^+(1s) + O^{5+}(1s^22s)$	ΔE_4=2.05
entrance	Φ_1	$He^{2+} + O^{4+}(1s^22s^2)$	

The main SEC process is the capture into 1s state of the He^+(1s) ion (exit channels Φ_4, Φ_{10}, Φ_{11} from Table I). The simultaneous capture and excitation (TE) of two electrons (exit channels Φ_5, Φ_{12}, Φ_{13}) in the He^{2+}–$O^{4+}(1s^2 2s^2)$ collision is an example of the correlation process. It was found that this TE process is of more importance than the electron capture into excited state of the He^+(2p) ion. The maximum value of the total SEC and TE processes was obtained to be equal $\sim 2.2\times 10^{-16}$ cm^2 at alpha-particle energy $\sim$ 0.7 MeV.

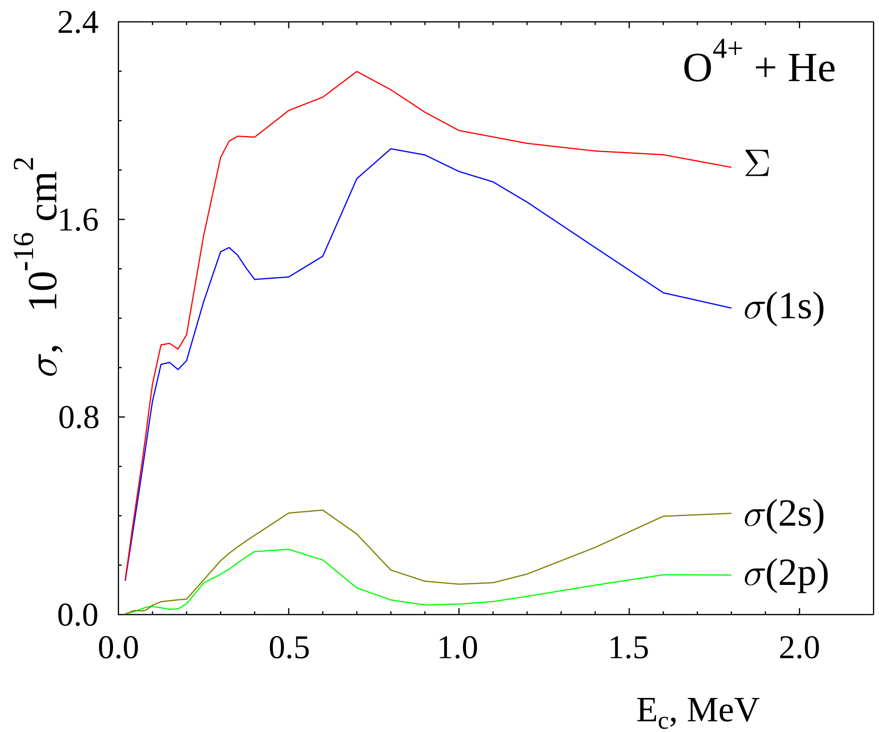

Figure 32: The total SEC + TE cross section Σ. The partial cross sections SEC+TE $\sigma(nl)$ of SEC into the nℓ-states of the He^+ ion with simultaneous electron 2s⟶2p excitation of target in the He^{2+} + O^{4+} collision. $\sigma(1s)$=σ_4 + σ_5, $\sigma(2s)$=σ_{10} + σ_{12}, $\sigma(2p)$=σ_{11} + σ_{13} (see Table I).

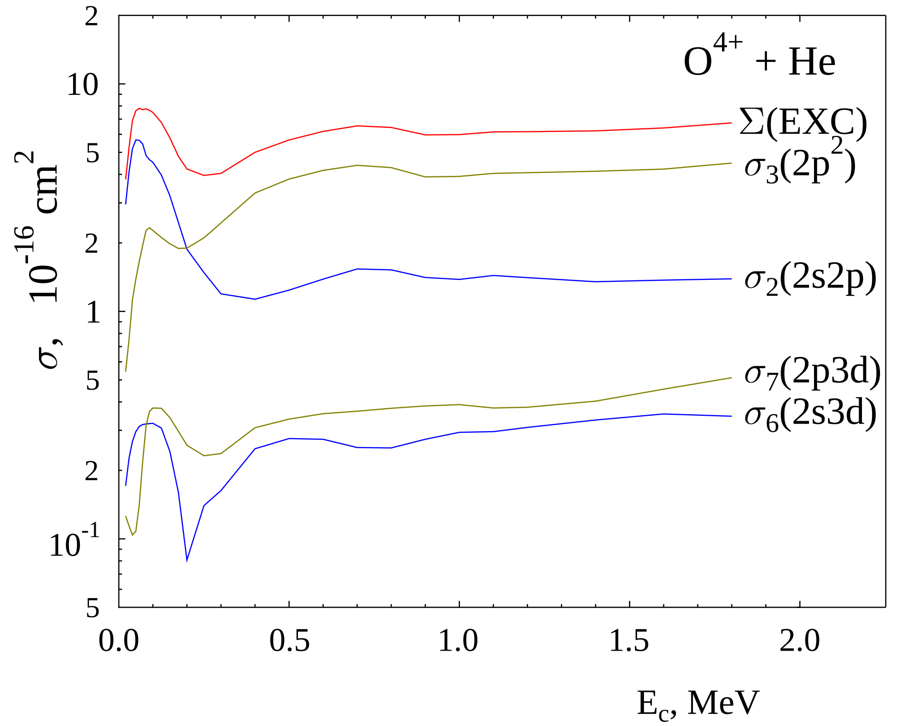

Figure 34: Cross sections of target excitation as a function of the collisional energy in the He^{2+}– O^{4+} collision: Σ_{exc} – the total cross section of excitation into $2\ell n\ell$ states with n=2,3 of the O^{4+} ions; σ_2(2s2p), σ_6(2s3d) – partial cross sections of the single-electron excitation into the 2s2p and 2s3d states of the O^{4+} ions (SE EXC, olive curves); $\sigma_3(2p^2)$, σ_7(2p3d) – partial cross sections of double-electron excitation into $2p^2$ and 2p3d states of the O^{4+} ions (DE EXC, blue curves).

The total excitation cross section as a function of the alpha particle energy has two humped structure. There is a maximum due to single-electron excitations ($\sim$ 7.7$\times 10^{-16}$ cm^2) at energy $\sim$ 80 keV and a feebly marked maximum ($\sim$ 6.5$\times 10^{-16}$ cm^2) at energy $\sim$ 0.7 MeV due to double-electron excitations.

8. Theoretical study of charge transfer and excitation in slow collisions between the Bi^{4+} ions in the ground and metastable states

We considered [7, 8] the processes of single-electron charge transfer and excitation occuring in collisions between the Bi^{4+} ions in the ground state in collisions between ions in the ground and metastable states for both the singlet and triplet entrance channels:

$$
{}^2\mathrm{S}\ \mathrm{Bi}^{4+}(6\mathrm{s}) + {}^2\mathrm{S}\ \mathrm{Bi}^{4+}(6\mathrm{s}) \rightarrow \begin{cases} {}^1\mathrm{S}\ \mathrm{Bi}^{3+}(6\mathrm{s}^2) + {}^1\mathrm{S}\ \mathrm{Bi}^{5+}(5\mathrm{d}^{10}), & \Delta\mathrm{E} = 11.16\ \mathrm{eV} \quad (1a) \\ {}^3\mathrm{P}\ \mathrm{Bi}^{3+}(6\mathrm{s}6\mathrm{p}) + {}^1\mathrm{S}\ \mathrm{Bi}^{5+}(5\mathrm{d}^{10}), & \Delta\mathrm{E} = 21.15\ \mathrm{eV} \quad (1b) \\ {}^2\mathrm{P}\ \mathrm{Bi}^{4+}(6\mathrm{p}) + {}^2\mathrm{S}\ \mathrm{Bi}^{4+}(6\mathrm{s}), & \Delta\mathrm{E} = 10.71\ \mathrm{eV.} \quad (1c) \end{cases}
$$

$$
{}^2\mathrm{S}\ \mathrm{Bi}^{4+}(6\mathrm{s}) + {}^2\mathrm{P}\ \mathrm{Bi}^{4+}(6\mathrm{p}) \rightarrow \begin{cases} {}^{1,3}\mathrm{P}\ \mathrm{Bi}^{3+}(6\mathrm{s}6\mathrm{p}) + {}^1\mathrm{S}\ \mathrm{Bi}^{5+}(5\mathrm{d}^{10}), & \Delta\mathrm{E} = 10.44\ \mathrm{eV} \quad (2a) \\ {}^1\mathrm{S}\ \mathrm{Bi}^{3+}(6\mathrm{s}^2) + {}^1\mathrm{S}\ \mathrm{Bi}^{5+}(5\mathrm{d}^{10}), & \Delta\mathrm{E} = 0.46\ \mathrm{eV} \quad (2b) \\ {}^2\mathrm{P}\ \mathrm{Bi}^{4+}(6\mathrm{p}) + {}^2\mathrm{S}\ \mathrm{Bi}^{4+}(6\mathrm{s}), & \Delta\mathrm{E} = 0 \quad (2c) \end{cases}
$$

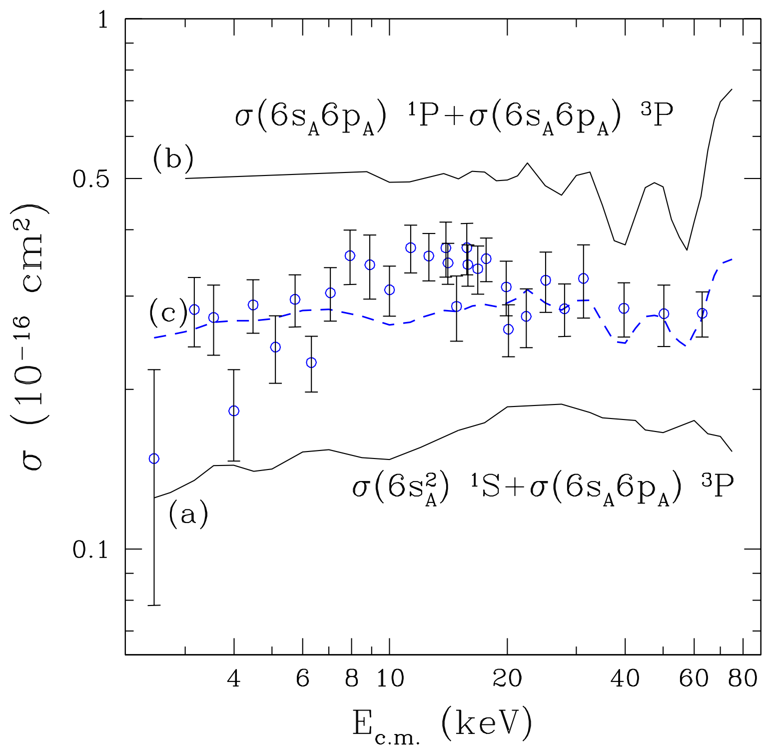

Figure 35: The statistically weighted total charge transfer cross sections for the singlet and triplet exit channels in (a) Bi^{4+}(6s)-Bi^{4+}(6s) and (b) Bi^{4+}(6s)-Bi^{4+}(6p) collisions. (c) The weighted average charge transfer cross section for fractions of reactions (a) and (b) of 0.6 and 0.4 – dashed line. (○) Total transfer cross section obtained in crossed-beam experiments [27].

Results obtained

The cross sections of processes under consideration have been calculated by the close-coupling equation method with the basis of two electron quasimolecular states (see Fig. 34 – $E_{\mathrm{c.m.}}$ is the center of mass collision energy). It has been found that SEC into the singlet states of the ^1S $Bi^{3+}(6s^2)$ ions makes a major contribution to the cross section for the $Bi^{4+}(6s)+Bi^{4+}(6s)$ collisions, whereas SEC into the singlet states ^1P $Bi^{3+}(6s6p)$ is the basic contribution to the cross section in the $Bi^{4+}(6s)+Bi^{4+}(6p)$ collisions.
The fraction of metastable ions in the beams has been estimated by comparing theoretical and experimental results for the charge transfer total cross sections. The dashed line in Fig. 34 refers to the charge transfer total cross section in the case when fractions of reactions 1 and 2 are 0.6 and 0.4 respectively. Such a proportion implies that the fraction of metastable ions amounts to 20% in either of crossed beams.

Other relevant literature references

[16] R. D. Piacentini, A. Salin, Computer Phys. Comm. 12, 199 (1976).

[17] V. K. Nikulin, N. A. Guschina. Diabatic correlation diagrams for quasimolecular description of ion-atom collisions. J. Phys. B: Atom and Molec. Phys. 11, 3553 (1978).

[18] W. Fritsch. APID 6, 131 (1995).

[19] R.K. Janev, E.A. Solov'ev, J.A. Stephens. State-Selective and Total Electron Capture, Excitation and Ionization Cross Sections in Slow Collisions of H(2s) and He^{+}(2s) with H^{+}, He^{2+}, Li^{3+}, Be^{4+}, and B^{5+}. IAEA, INDC(NDS)-393, 1999, Vienna.

[20] W. Fritsch and H. Tawara. Present Status on Atomic and Molecular DATA Relevant to Fusion Plasma and Modeling. NIFS–DATA–39, 1997, p.89.

[21] L. Salasnich, F. Sattin, Phys. Rev. A 51 (1995) 4281.

[22] H.Tawara. Roles of Atomic and Molecular Processes in Fusion Plasma Researches. NIFS–DATA–25, 1995.

[23] D. H. Crandall, Phys. Rev. A 16, 958 (1977).

[24] M. Kimura and R. E. Olson, J. Phys. B: Atom. Mol. Phys. 17, 713 (1984).

[25] L. F. Errea, B. Herrero, L. Mendes and A. Riera, J. Phys. B: Atom. Mol. Phys. 28, 693 (1995).

[26] R. A. Phaneuf and D. H. Crandall, 1981.

[27] A. Diehl, H. Brauning, R. Trassl, D. Hathiramani, A. Theiss, H. Kern, E. Salzborn, and I. Hofmann, J Phys. B 34, 4073 (2001).